CHAPTER ONE

SALEN-SUPPORTED COBALT CATALYSTS FOR STEREO- AND REGIOSELECTIVE EPOXIDE/CO_2 COPOLYMERIZATION

1.1 Introduction

In 1969, Inoue and coworkers discovered a 1:1 $Zn(CH_2CH_3)_2/H_2O$ heterogeneous catalyst for propylene oxide (PO)/CO_2 copolymerization, yielding poly(propylene carbonate) (PPC).[1] Notably, CO_2 is an ideal synthetic feedstock as it is non-toxic, inexpensive, and readily available.[2] Furthermore, PPC is an attractive material for thermally reversible binders, adhesives, and coatings due to its low glass transition temperature ($T_g \approx 40$ °C) and clean thermal decomposition ($T_d \approx 220$ °C) (Figure 1.1).[3] The $Zn(CH_2CH_3)_2/H_2O$ system, however, generates PPC with a high polyether content (poly(propylene oxide) or PPO) and the byproduct propylene carbonate (PC) is also formed in significant quantities, limiting the utility of this reaction (Scheme 1.1).[1]

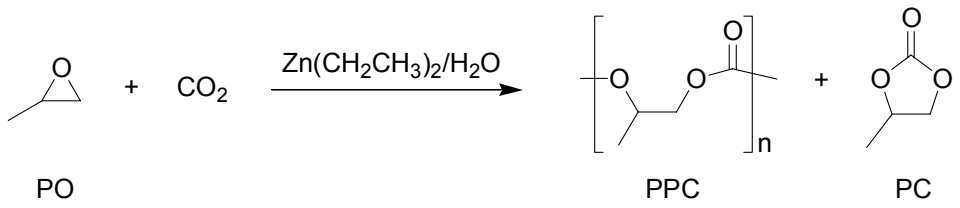

Scheme 1.1. $Zn(CH_2CH_3)_2/H_2O$ catalysts for PO/CO_2 copolymerization yielding PPC and PC.

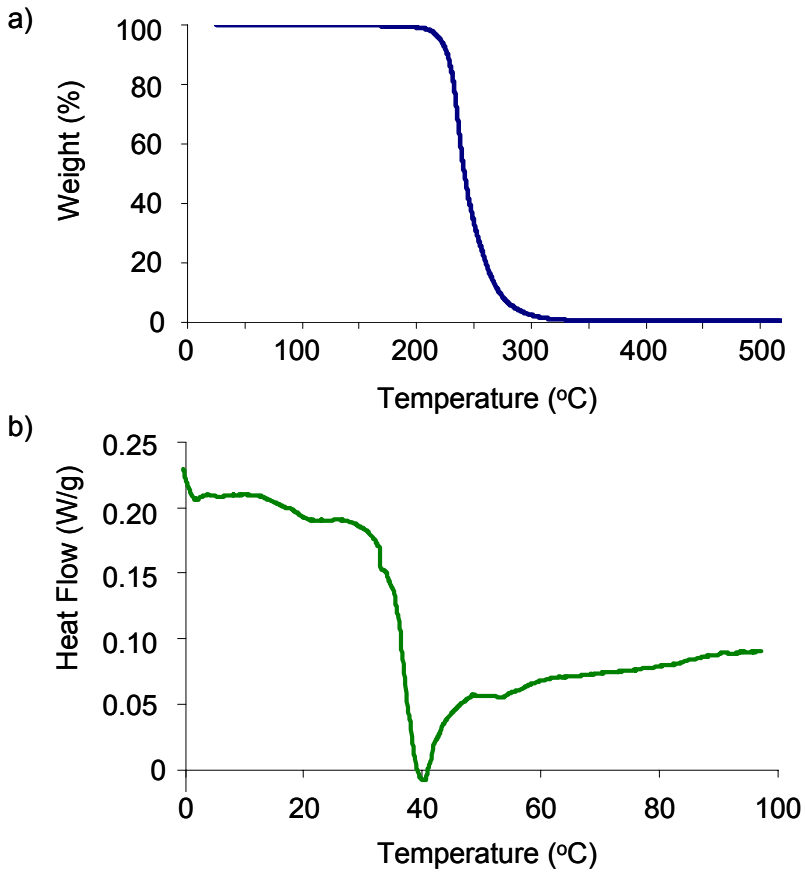

Figure 1.1. a) Thermogravimetric analysis (TGA) and b) differential scanning calorimetry (DSC) of regioregular, atactic PPC.

Since Inoue's pioneering work, numerous research efforts have focused on catalysts for epoxide/CO_2 copolymerization with the common goals of increasing reaction rates, improving selectivity for polymer over cyclic carbonate, maximizing carbonate incorporation, and controlling polymer microstructure.[4] Initially, heterogeneous systems similar to those used by Inoue were developed; however, the most significant advances were accomplished using homogeneous catalysts. Notably, these discrete complexes contain a tunable active site and are more amenable to mechanistic study.

The application of homogeneous zinc-based bis(phenoxide) or *β*-diiminate catalysts for epoxide/CO_2 copolymerization realized increased reaction rates for highly alternating polycarbonate with controlled molecular weight.[4, 5] The polymers generated with these systems, however, were generally *regioirregular* and *atactic* (Figure 1.2). In the case of PO/CO_2 copolymerization, competing backbiting mechanisms leading to PC formation remained a problem (Scheme 1.2).[6]

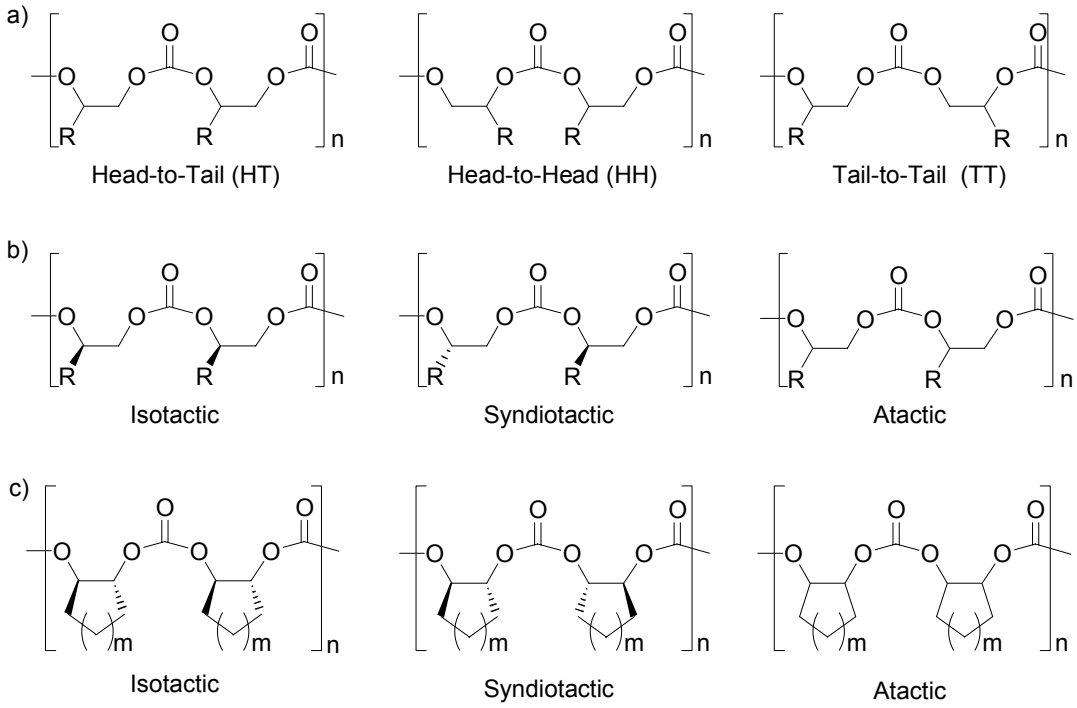

Figure 1.2. General classifications of polycarbonates: a) regiochemistry of aliphatic polycarbonates, b) stereochemistry of regioregular, aliphatic polycarbonates, and c) stereochemistry of alicyclic polycarbonates.

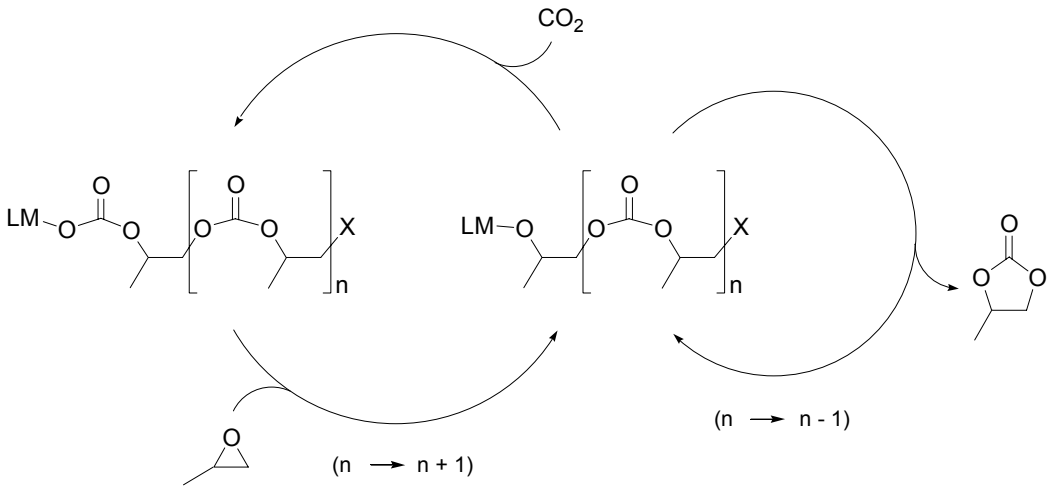

Scheme 1.2. PO/CO_2 copolymerization using discrete metal (LM) alkoxides (X = OR) and carboxylates ($X = O_2CR$).

Through careful modulation of ligand structure and reaction conditions, we observed selectivities up to 93% for PPC over PC using zinc *β*-diiminate catalysts bearing an electron withdrawing (CF_3) functionality.[6] Meanwhile, both we, and Nozaki applied a chiral ligand framework, affording the first examples of stereoselective CHO/CO_2 copolymerization (Figure 1.3).[7-11] With these systems, *isotactic* poly(cyclohexene carbonate) (PCHC) with an enantiomeric excess (*ee*) > 70% was synthesized.

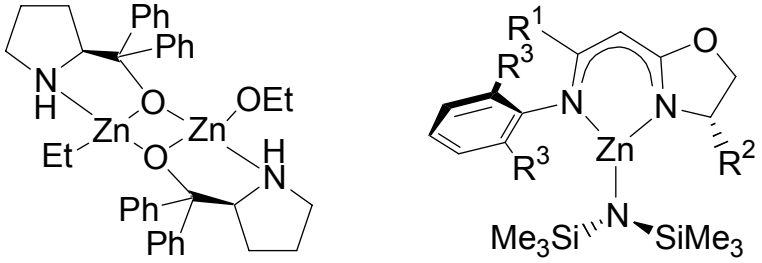

Figure 1.3. Catalysts for the isospecific copolymerization of CHO and CO_2; R^1 = Me, CF_3, or ^{i}Pr; R^2 = (*R*)-Ph, (*S*)-^{i}Pr, or (*S*)-^{t}Bu; R^3 = Et or ^{i}Pr.

As an alternative to zinc-based systems, metal porphyrins in combination with Lewis basic or organic-based, ionic cocatalysts were applied to the coupling of epoxides and CO_2.[4] Notably, these systems provided for the first examples of monodisperse polycarbonates with narrow MWDs and in some cases demonstrated "immortal"-type behavior.[12] More recently, Jacobsen and coworkers' groundbreaking work using chiral (salen)M (salen = *N,N′*-bis(salicylidene)-1,2-diaminoalkane) complexes for the asymmetric ring opening and kinetic resolution of epoxides[13] inspired the pursuit of similar catalysts for epoxide/CO_2 copolymerization (Figure 1.4). Specifically (salen)MX (M = Cr, Co; X = nucleophile or counterion) complexes have achieved the highest activities for PO/CO_2 copolymerization with near perfect selectivity for PPC over PC.[14-24] Generally, the most elevated turnover frequencies (TOF)s result through application of an organic-based ionic,[19-22, 24-28] or Lewis basic cocatalyst;[15-18, 21-24, 27, 29-31] a similar effect observed with the previously studied porphyrin-supported systems.[4] Furthermore, the role of these cocatalysts in the epoxide/CO_2 copolymerization is a subject of ongoing mechanistic study.

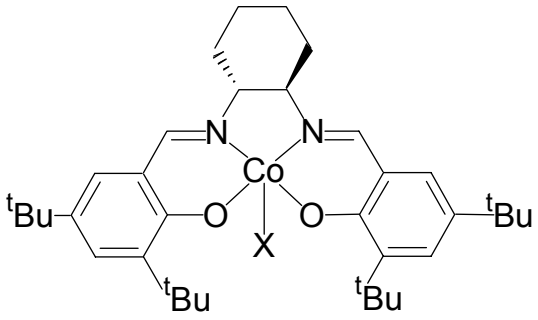

Figure 1.4. (*R,R*)-(Salcy)CoX (X = nucleophile or counterion) complexes for epoxide/CO_2 copolymerization.

Table 1.1. Summary of PPC and PCHC microstructures synthesized.[a]

Catalyst	Cocatalyst	Epoxide	Polycarbonate Regiochemistry[b]	Polycarbonate Stereochemistry[b]
(*R,R*)-(salcy)CoBr	None	*rac*-PO	regioregular	atactic
(*R,R*)-(salcy)CoBr	None	(*S*)-PO	regioregular	isotactic
(*R,R*)-(salcy)CoBr	None	(*R*)-PO	regioirregular	heterotactic
rac-(salcy)CoBr	None	*rac*-PO	regioregular	syndioenriched
(*R,R*)-(salcy)CoOBzF_5	[PPN]Cl	*rac*-PO	regioregular	isoenriched
rac-(salen-**3**)CoBr	None	CHO	NA	syndiotactic
(*R,R*)-(salcy)CoOBzF_5	[PPN]Cl	CHO	NA	atactic
(*R,R*)-(salen-**5**)CoBr	None	CHO	NA	isotactic

[a] [PPN]Cl = bis(triphenylphosphine)iminium chloride, (salcy) = *N,N′*-bis(3,5-di-*tert*-butylsalicylidene)-1,2-diaminocyclohexane, (salen-**3**) = *N,N′*-bis(3,5-di-*tert*-butylsalicylidene)-1,2-diaminopropane, (salen-**5**) = *N,N′*-bis(3,5-di-α,α'-dimethylbenzylsalicylidene)-1,2-diaminocyclohexane. [b] Determined by $^{13}C\{^1H\}$ NMR spectroscopy.

Herein, we review our work concerning the use of chiral and racemic (salcy)CoX (salcy = *N,N′*-bis(3,5-di-*tert*-butylsalicylidene)-1,2-cyclohexanediimine; X = halide or carboxylate) complexes with and without organic-based ionic, and Lewis basic cocatalysts for stereo- and regioselective PO/CO_2 copolymerization.[14, 19, 22] Additionally, we describe stereoselective CHO/CO_2 copolymerization using a series of chiral, racemic and achiral (salen)CoX (X = halide or carboxylate) catalysts.[28] With

these systems, we observe catalytic activities up to three orders of magnitude faster than those of the original heterogeneous zinc-based systems. Furthermore, we have synthesized unprecedented microstructures for both PPC and PCHC which has led to new mechanistic consideration (Table 1.1).

1.2 (Salcy)CoX catalysts for regio- and stereoselective PO/CO_2 copolymerization

The copolymerization of PO and CO_2 with discrete metal complexes has been well documented.[4] Notably, β-diiminate zinc or salen-type chromium catalysts with cocatalysts have resulted in the highest reported activities for this reaction but produce regioirregular PPC with significant quantities of PC in most cases.[6, 15-17, 23, 24]

With the goals of improving selectivity for PPC over PC and controlling PPC microstructure, we proceeded to investigate metal/ligand combinations known to effect stereo- and regioselective reactions with PO. Jacobsen and coworkers have reported chiral (salcy)Co^{III} carboxylates for the hydrolytic kinetic resolution of epoxides with remarkable efficiencies.[13] When we applied (*R,R*)-(salen)CoOAc to *rac*-PO/CO_2 copolymerization, we observed unprecedented selectivity for highly regioregular PPC.[14] Specifically, (*R,R*)-(salcy)CoOAc generated PPC with 99% carbonate linkages and 83% head-to-tail (HT) connectivity, with no observable PC (Table 1.2, entry 1). Furthermore, with this system, we calculate a k_{rel} = 2.8, with a preference for (*S*)- over (*R*)-PO. To our knowledge, this was the first example of a regioselective *rac*-PO/CO_2 copolymerization catalyst, however, the (*R,R*)-(salcy)CoOAc system was significantly less active than the zinc- and chromium-based alternatives, and required high CO_2 pressures and moderate temperatures (22 °C).

Initial studies using catalyst (*R,R*)-(salcy)CoOAc afforded PPCs with low number average molecular weights (M_n)s and broad molecular weight distributions (MWD)s. Through careful elimination of all chain transfer agents, such as water, PPC

with a measured M_n that agrees more closely with the theoretical value is obtained (Table 1.2, entry 2).[19]

Table 1.2. (*R,R*)-(Salcy)CoX (X = OAc, Br) catalyzed copolymerization of *rac*-, (*S*)-, and (*R*)-PO/CO_2.[a]

Entry	Axial Ligand X =	PO	PPC Yield[b] (%)	TOF[c] (h^{-1})	M_n[d] (kg/mol)	M_w/M_n[d]	Head-to-Tail Linkages[e](%)
1[f]	OAc	*rac*	25	62	10.4[g]	1.31	83
2	OAc	*rac*	30	74	15.5	1.16	83
3	Br	*rac*	36	89	21.0	1.14	82
4	Br	(*S*)	49	120	20.1	1.21	93
5	Br	(*R*)	20	50	13.3	1.16	43

[a] Copolymerizations run neat with [PO]:[Co] = 500:1 at 22 °C for 2 h with 800 psi of CO_2. Selectivity for PPC over PC is > 99:1, PPC contains ≥ 96% carbonate linkages as determined by ^{1}H NMR spectroscopy ($CDCl_3$, 300 MHz). [b] Based on isolated PPC yield. [c] Turnover frequency for PPC = (mol PO/(mol Co · h)). [d] Determined by GPC calibrated with polystyrene standards in THF at 40 °C. [e] Determined by quantitative $^{13}C\{^1H\}$ NMR spectroscopy ($CDCl_3$, 125 MHz, d_1 = 10s). [f] Ambient reaction conditions. [g] M_n averaged over a bimodal GPC distribution.

In an effort to uncover a more active *rac*-PO/CO_2 copolymerization catalyst, we proceeded to investigate a series of (*R,R*)-(salcy)CoX complexes with various axial ligands, X. The (*R,R*)-(salcy)CoX (X = halide or carboxylate) catalyzed *rac*-PO/CO_2 copolymerization results are pictured in Figure 1.5. Although the overall performance of (*R,R*)-(salcy)CoOAc and (*R,R*)-(salcy)CoOBzF_5 (OBzF_5 = pentafluorobenzoate) proved largely similar, use of the various halides [(*R,R*)-(salcy)CoCl, (*R,R*)-(salcy)CoBr, or (*R,R*)-(salcy)CoI] resulted in substantial changes in catalytic activity.

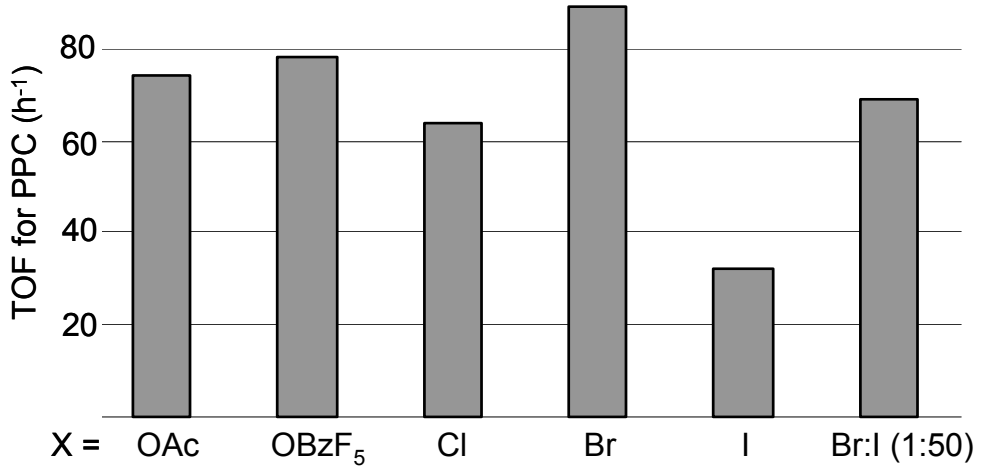

Figure 1.5. Effect of catalyst (*R,R*)-(salcy)CoX axial ligand, X, on *rac*-PO/CO_2 copolymerization rate. Copolymerizations run neat with [*rac*-PO]:[Co] = 500:1 at 22 °C for 2 h with 800 psi of CO_2. In all cases, selectivity for PPC over PC is > 99:1, PPC contains ≥ 96% carbonate linkages with M_w/M_n < 1.25, and ≥ 81 % HT connectivity.

The order of increasing activity for copolymerization with (*R,R*)-(salcy)CoX complexes is X = I < Cl < OAc ≈ $OBzF_5$ < Br, with the most active catalyst, (*R,R*)-(salcy)CoBr, producing PPC with a TOF of 89 h^{-1}. Interestingly, through combination of as little as 2% of the more active (*R,R*)-(salcy)CoBr with catalyst (*R,R*)-(salcy)CoI yielded a TOF of 69 h^{-1}; a copolymerization rate more than double that of unassisted (*R,R*)-(salcy)CoI, even though [I^-]:[Br^-] is 50:1. We suspect that this is a result of a bimetallic initiation, similar to that proposed by Jacobsen and coworkers for the hydrolytic kinetic resolution of epoxides (Scheme 1.3)[32] and by Darensbourg and coworkers concerning salen-supported chromium systems for CHO/CO_2 copolymerization.[27]

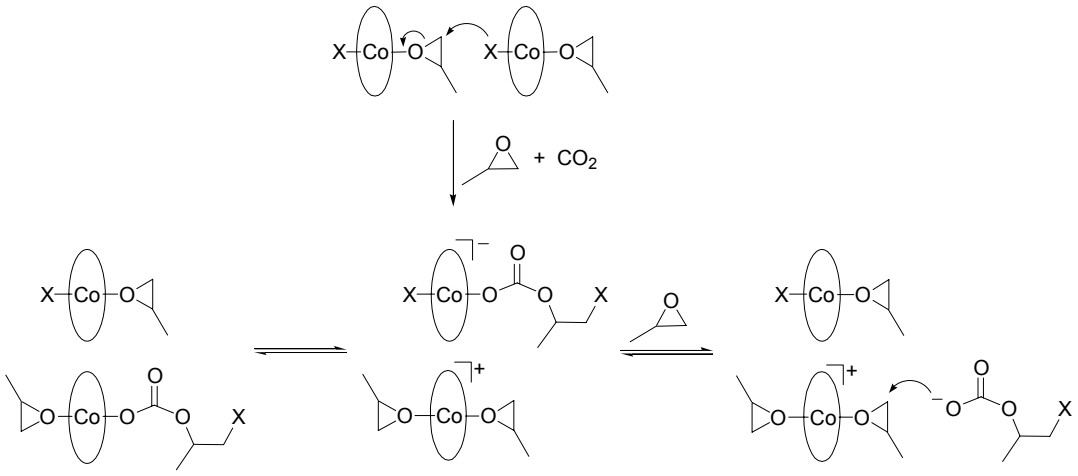

Scheme 1.3. Bimetallic initiation and propagation leads to PPC formation (X = halide, carboxylate, or polymer).

The preference for (*S*)- over (*R*)-PO using catalyst (*R,R*)-(salcy)CoOAc inspired us to compare the copolymerization of *rac*-, (*S*)-, and (*R*)-PO/CO_2 using the more active (*R,R*)-(salcy)CoBr catalyst. The PPC generated from the *rac*-PO/CO_2 copolymerization is regioregular and atactic as determined from the corresponding $^{13}C\{^1H\}$ NMR spectrum (Figure 1.6a and Table 1.2, entry 3) Replacing *rac*- with (*S*)-PO, increases the catalytic activity of (*R,R*)-(salcy)CoBr from 89 to 120 turnovers per hour, for isotactic PPC with 93% HT connectivity (Figure 1.6b and Table 1.2, entry 4). Degradation of this polymer to PC while conserving all stereocenters[33] yields a (*S*)-PC:(*R*)-PC ratio of 97:3 as determined by gas chromatography, consistent with PO ring opening at the methylene carbon with stereochemical retention.

When (*R*)-PO is used in place of *rac*-PO, catalytic activity of (*R,R*)-(salcy)CoBr decreases to 50 turnovers per hour and the resultant PPC is almost perfectly regiorandom with 43% HT connectivity (Figure 1.6c and Table 1.2, entry 4). In this case, degradation of the polymer to PC yields a (*S*)-PC:(*R*)-PC ratio of 34:66.

The excess of (*R*)-stereocenters in the PPC reflects that the generation of a HH linkage through misinsertion is most often immediately corrected to generate a TT linkage, followed by the incorporation of a couple of (*R*)-HT linkages until the next regioerror occurs.

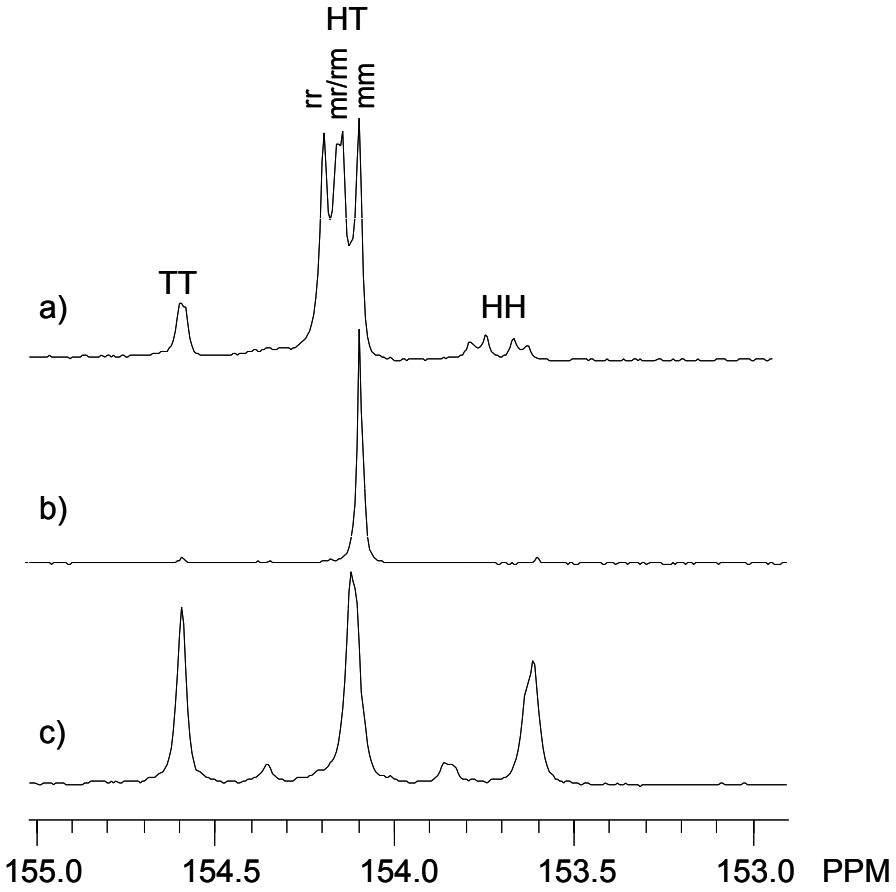

Figure 1.6. Carbonyl region of the quantitative $^{13}C\{^{1}H\}$ NMR ($CDCl_3$, 125 MHz, d_1 = 10s) spectra of (a) regioregular, atactic PPC synthesized from (*R,R*)-(salcy)CoBr and *rac*-PO/CO_2 (b) regioregular, isotactic PPC synthesized from (*R,R*)-(salcy)CoBr and (*S*)-PO/CO_2, and (c) regioirregular PPC synthesized from (*R,R*)-(salcy)CoBr and (*R*)-PO/CO_2.

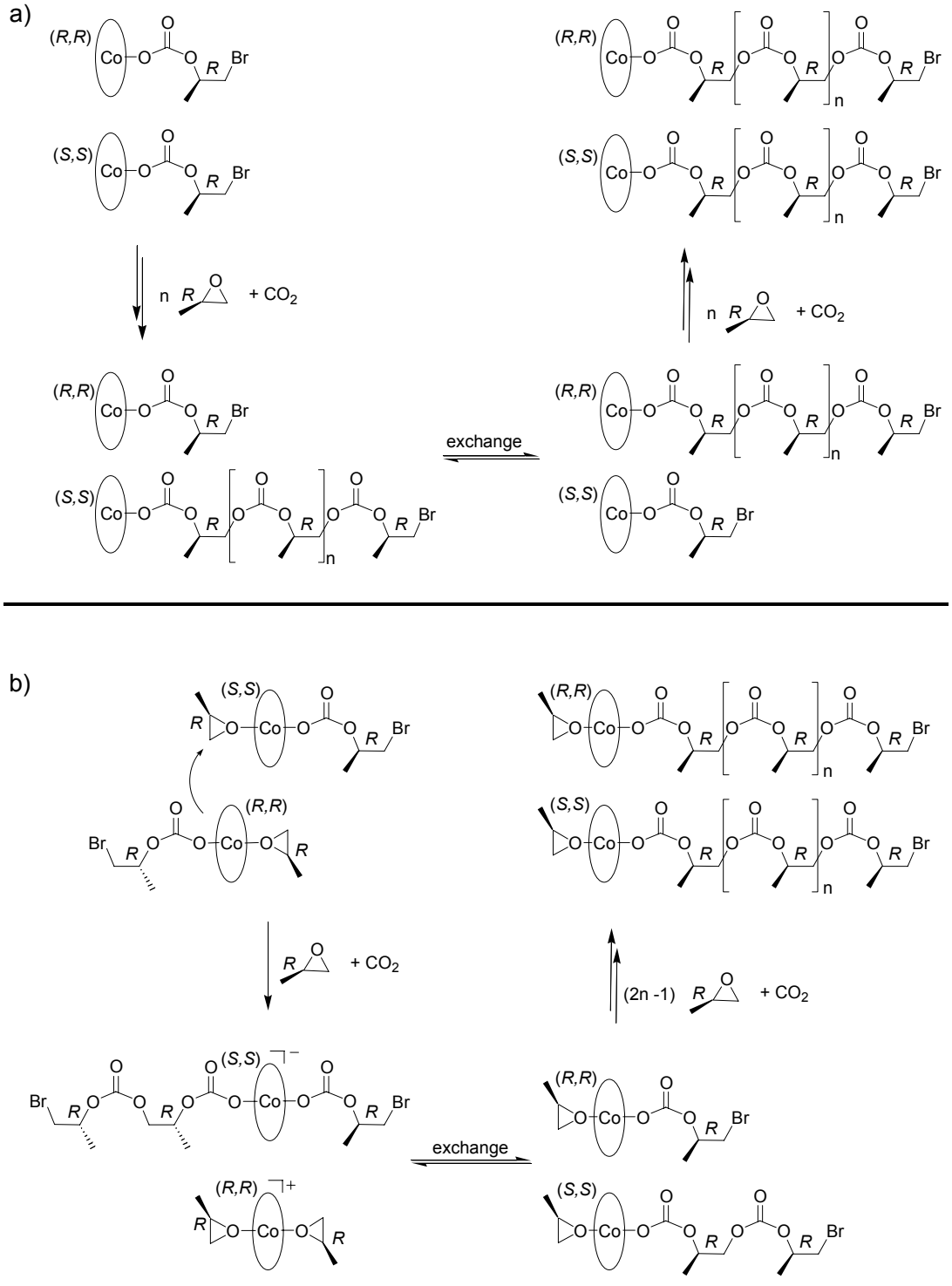

Scheme 1.4. The propagating carboxylate a) rapidly exchanges between metal centers, where (*R*)-PO ring opening is favored on the (*S,S*)-complex b) via a bimetallic propagation mechanism.

In order to uncover how the propagating species is influenced by catalysts of both possible chiralities we applied the racemic catalyst, *rac*-(salcy)CoBr, to PO/CO_2 copolymerization. Unexpectedly, the copolymerization of (*R*)-PO and CO_2 with *rac*-(salcy)CoBr yielded a regioregular, isotactic PPC (MWD = 1.16) with a catalytic activity of 100 turnovers per hour. Notably, no distinction in activity between the (*S,S*)- and (*R,R*)-(salcy)CoBr catalysts with (*R*)-PO was observed. We suggest that the propagating carboxylate dissociates from the catalyst during the copolymerization and rapidly exchanges between metal centers, where the (*R*)-PO ring opening is favored on the (*S,S*)-complex (Scheme 1.4).

When we carried out the *rac*-PO/CO_2 copolymerization with catalyst *rac*-(salcy)CoBr, to our surprise, the product PPC had an unprecedented $^{13}C\{^1H\}$ NMR spectrum. In this case, a large HT [*rr*] tetrad resonance exceeded that of the remaining HT [*mr*], [*rm*], and [*mm*] shifts (Figure 1.7) We again put forth that the propagating carboxylate dissociates from the cobalt center and rapidly exchanges between metal centers, however, in this case the stereocenter on the propagating chain-end also influences the site at which enchainment of (*S*)- and (*R*)-PO occurs (Scheme 1.5).[34]

In summary, complexes (salcy)CoX are active catalysts for PO/CO_2 copolymerization yielding highly alternating, regioregular PPC with controlled molecular weight and no detectable PC. By varying the relative catalyst and PO stereochemistry, we observed pronounced alterations in catalyst activity and PPC microstructure. This has led to the synthesis of syndio-enriched PPC, a previously unreported microstructure.

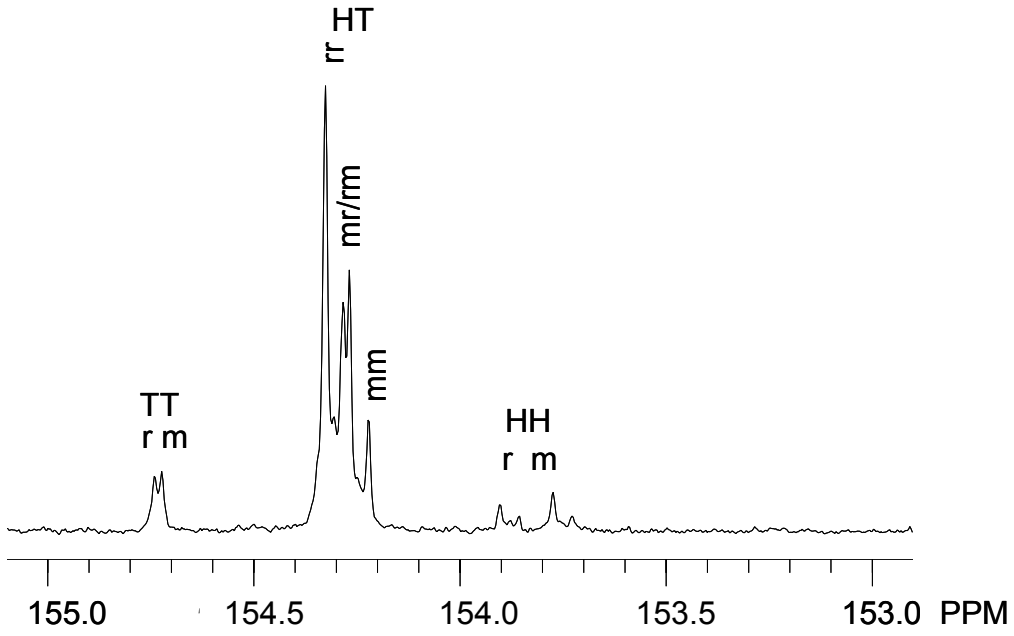

Figure 1.7. Carbonyl region of the quantitative $^{13}C\{^{1}H\}$ NMR ($CDCl_3$, 150 MHz, d_1 = 10s) spectrum of syndiotactic PPC synthesized from *rac*-(salcy)CoBr and *rac*-PO/CO_2.

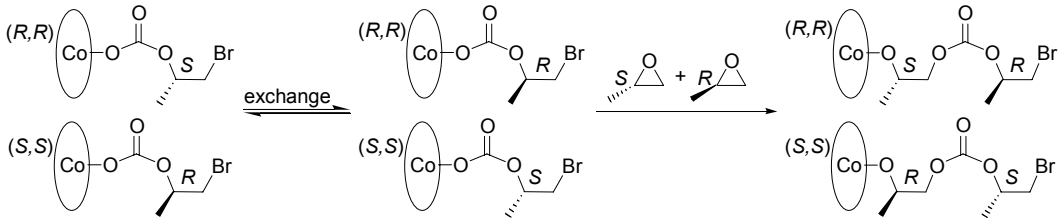

Scheme 1.5. The propagating carboxylate rapidly exchanges between metal centers. This exchange occurs in conjunction with a chain-end control mechanism with alternate enchainment of (*S*)- and (*R*)-PO.

1.3 Addition of cocatalyst [PPN]Cl

The coupling of porphyrin or salen-type metal catalysts with organic-based, ionic cocatalysts has resulted in improved catalytic activities in a variety of polymerization systems.[19-22, 24-28] The addition of ammonium-based, ionic cocatalysts (*n*-Bu_4NY; Y = Cl, Br, I) to (*R,R*)-(salcy)CoX (X = OAc, O_2CCCl_3, O_2CCF_3, Cl, OTs; Ts = *p*-toluenesulfonyl) in the presence of PO and CO_2, shows reaction rates that are sensitive to the anionic components (X and Y) for the generation of PC.[35] Although it was originally thought that ammonium-based, ionic cocatalysts limited the (*R,R*)-(salcy)CoX catalyzed reaction of PO/CO_2 to the production of PC, PPC was recently achieved through the careful choice of the complex and cocatalyst.[20, 21] Specifically, (*R,R*)-(salcy)CoOAr (Ar = 4-nitrophenyl, 2,4-dinitrophenyl, or 2,4,6-trinitrophenyl) derivatives with [*n*-Bu_4N]Y (Y = Cl, OAc) cocatalysts were described by Lu and coworkers to afford PPC with exceptional rates and selectivity. The most successful cocatalyst consists of a quaternary ammonium cation and an anion that is a good nucleophile with a poor leaving ability. Since our discovery of the active (*R,R*)-(salcy)CoOAc system, we have furthered catalyst optimization, which has led to the use of organic-based, ionic cocatalysts similar to those reported by Inoue, Darensbourg, and Lu.[20, 21, 24-27]

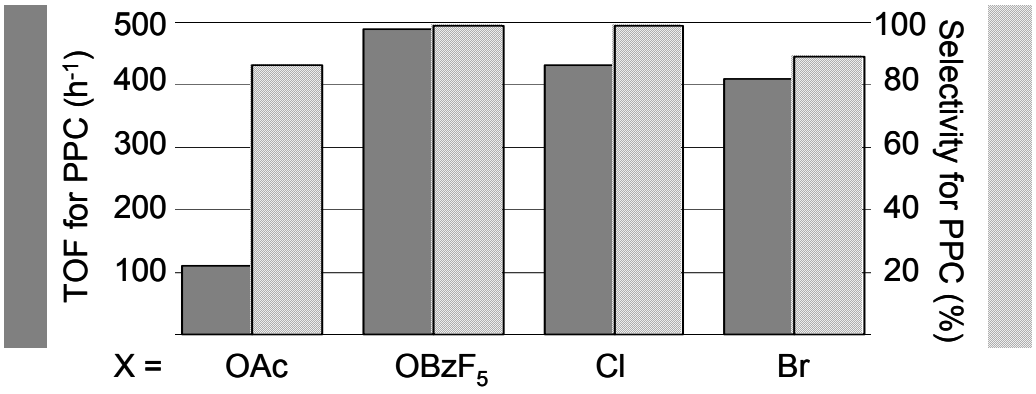

Figure 1.8. Effect of catalyst (*R,R*)-(salcy)CoX axial ligand, X, on *rac*-PO/CO_2 copolymerization rate using cocatalyst [PPN]Cl. Copolymerizations run neat with [*rac*-PO]:[Co]:[[PPN]Cl] = 2000:1:1 at 22 °C for 2 h with 200 psi of CO_2. PPC contains ≥ 98% carbonate linkages with $M_w/M_n \leq 1.15$ and ≥ 93% HT connectivity. Turnover frequency for PPC = (mol PO/(mol Co · h)). Selectivity for PPC = selectivity for PPC over PC.

Initially, we added [PPN]Cl, a commercially available, readily dried (hydrophobic) ionic compound with a bulky cation and a nucleophilic anion, to the (*R,R*)-(salcy)CoX (X = halide or carboxylate) catalyzed *rac*-PO/CO_2 copolymerization. We observed a remarkable improvement in catalytic activity when [PPN]Cl was combined with any of the (*R,R*)-(salcy)CoX complexes for highly alternating, regioregular PPC (Figure 1.8). Furthermore, these catalyst systems showed the highest activities at low CO_2 pressures (50 – 200 psi); a result quite different from the analogous (salcy)CoX complexes alone. The most active catalyst system, (*R,R*)-(salcy)CoOBzF_5/[PPN]Cl, exhibited a TOF > 600 h^{-1} for PPC with 94% HT connectivity and only 1% PC byproduct. Notably, the most active and selective (*R,R*)-(salcy)CoX/[PPN]Cl catalyst system contains an axial ligand that is concurrently a good nucleophiles and a poor leaving group. Catalyst (*R,R*)-(salcy)CoOAc/[PPN]Cl

had the lowest activity of all of the (salcy)CoX/[PPN]Cl systems, which we attribute to its poor solubility in the PO/CO_2 reaction mixture at low CO_2 pressures.

Although (*R,R*)-(salcy)CoOBzF_5/[PPN]Cl selectively couples PO and CO_2 to form PPC and not PC, after extended reaction times the overall selectivity for polymer decreases (Table 1.3, entries 1 - 3). We observe at approximately 50% conversion, the polymerization solidifies, and the PPC depolymerizes in situ to form PC; a pathway only observed when the copolymerization is run neat.

Table 1.3. (*R,R*)-(Salcy)CoOBzF_5/[PPN]Cl catalyzed *rac*-, (*S*)-, and (*R*)-PO/CO_2 copolymerization.[a]

Entry	PO	Time (h)	PPC Yield[b] (%)	TOF[c] (h^{-1})	Selectivity[d] (PPC:PC)	M_n[e] (kg/mol)	M_w/M_n[e]	Head-to-Tail Linkages[f] (%)
1	*rac*	1.0	32	640	99:1	26.8	1.13	94
2	*rac*	2.0	49	490	>99:1	43.0	1.10	93
3	*rac*	6.0	59	200	56:46	41.4	1.36	93
4	(*S*)	0.5	27	1,100	>99:1	22.2	1.15	96
5	(*R*)	2.0	21	210	98:2	19.1	1.12	87

[a] Copolymerizations run neat with [PO]:[(*R,R*)-(salcy)CoOBzF_5]:[[PPN]Cl] = 2000:1:1 at 22 °C with 200 psi of CO_2. PPC contains ≥ 98% carbonate linkages as determined by ^{1}H NMR spectroscopy ($CDCl_3$, 300 MHz). [b] Based on isolated PPC yield. [c] Turnover frequency for PPC = (mol PO/(mol Co · h)). [d] Selectivity for PPC over PC. [e] Determined by GPC calibrated with polystyrene standards in THF at 40 °C. [f] Determined by quantitative $^{13}C\{^1H\}$ NMR spectroscopy ($CDCl_3$, 125 MHz, d_1 = 10s).

The remarkable difference in activity and regioselectivity for *rac*-, (*S*)-, and (*R*)-PO/CO_2 copolymerization observed with (*R,R*)-(salcy)CoBr led us to pursue similar studies with the (*R,R*)-(salcy)CoOBzF_5/[PPN]Cl system. The *rac*-, (*S*)-, and (*R*)-PO/CO_2 copolymerization data for (*R,R*)-(salcy)CoOBzF_5/[PPN]Cl is presented in Table 1.3 and Scheme 1.6. As previously described, (*R,R*)-(salcy)CoOBzF_5/[PPN]Cl demonstrates an activity > 600 turnovers per hour for the copolymerization of *rac*-PO

and CO_2, affording regioregular, iso-enriched PPC (Table 1.3, entry 1 and Scheme 1.6a). Amazingly, the substitution of (*S*)- for *rac*-PO results in a near doubling of the reaction rate (TOF = 1100 h^{-1}), yielding regioregular, isotactic PPC (Table 1.3, entry 4 and Scheme 1.6b). Alternatively, the substitution of (*R*)- for *rac*-PO results in substantial rate inhibition with a TOF = 210 h^{-1} for isotactic, regioregular PPC (Table 1.3, entry 5 and Scheme 1.6c). Finally, when *rac*-(salcy)CoOBzF_5/[PPN]Cl is used, the (*R*)-PO/CO_2 copolymerization yields regioregular, isotactic PPC (Scheme 1.6d). Similar to the results observed with catalyst *rac*-(salcy)CoBr alone, this supports a mechanism where the propagating species dissociates from the metal center during the copolymerization and is influenced by catalysts of both possible chiralities. In contrast to the *rac*-(salcy)CoBr system in absence of [PPN]Cl, the *rac*-PO/CO_2 copolymerization catalyzed by *rac*-(salcy)CoOBzF_5/[PPN]Cl did not yield syndiotactic PPC, but instead has high activity for isotactic polymer (Scheme 1.6e). We consider that in the presence of [PPN]Cl, a chain-end control mechanism is no longer operable.

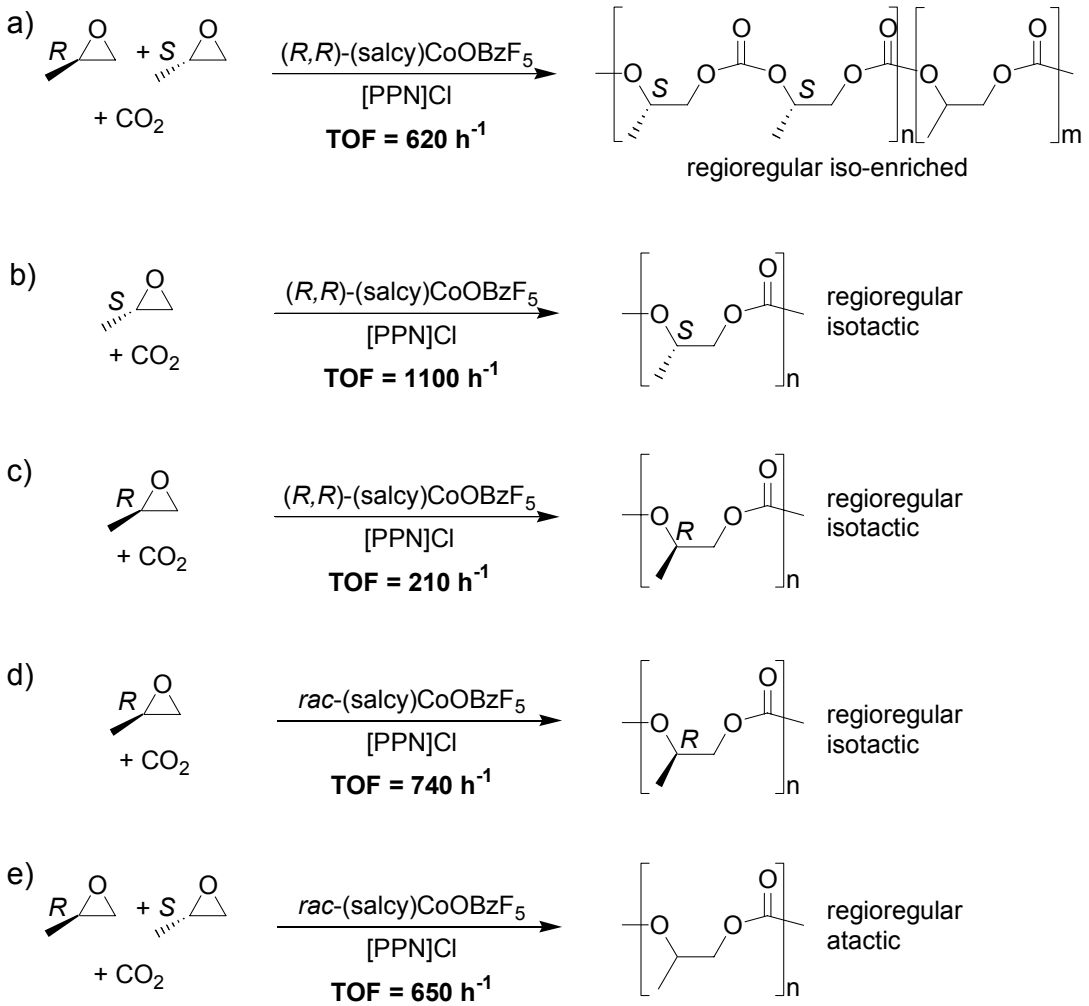

Scheme 1.6. The relative catalyst and monomer stereochemistry influence the catalyst activity and the microstructure of the PPC formed: (*R,R*)-(salcy)CoOBzF$_5$/[PPN]Cl for a) *rac*- b) (*S*)- and c) (*R*)-PO/CO_2 copolymerization. *rac*-(Salcy)CoOBzF$_5$/[PPN]Cl for d) (*R*)- and e) *rac*-PO/CO_2 copolymerization.

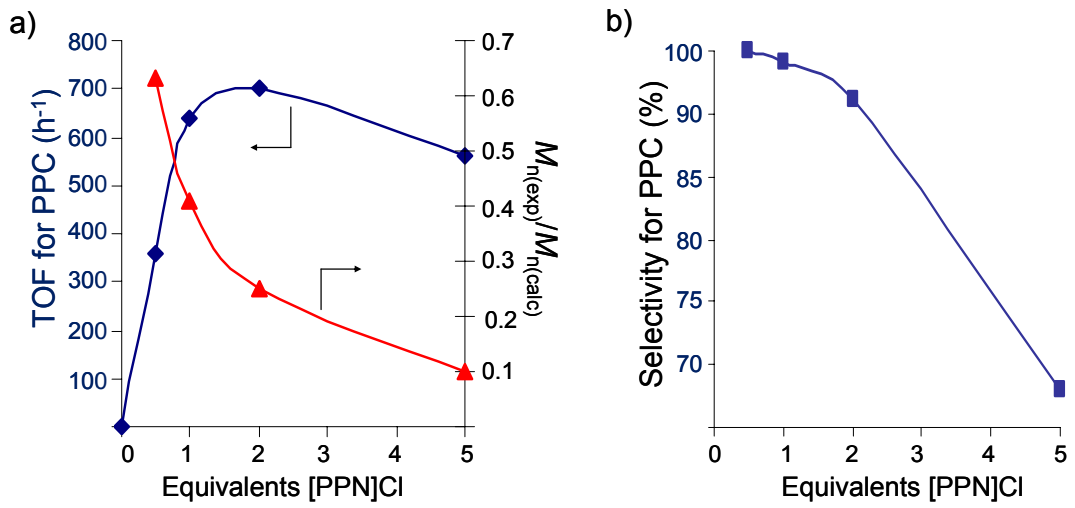

Figure 1.9. Relative [PPN]Cl cocatalyst loading influences a) catalyst activity, the M_n value of the PPC formed (M_n experimental/ M_n calculated) and b) selectivity for PPC over PC. Copolymerizations run neat at 22 °C with [*rac*-PO]:[(*R,R*)-(salcy)CoOBzF$_5$] = 2000:1 with 100 psi of CO_2. Reactions run to < 40% PPC conversion. $M_{n(exp)}/M_{n(calc)}$ = ratio of the experimental M_n value to the 7</VOLUME><NUMBER>31</NUM*B*ER><PAGES>1023

The PPCs obtained from the (*R,R*)-(salcy)CoOBzF$_5$/[PPN]Cl catalyzed PO/CO_2 copolymerization have M_n values equal to approximately half of the theoretical values based on conversion. We suspect that initiation involves both the axial ligand of the cobalt catalyst and the anion from the [PPN]$^+$-based cocatalyst. To test this possibility, we carried out the copolymerization with a constant [PO]:[Co] loading while varying the amount of [PPN]Cl. As predicted, as more [PPN]Cl is added to the copolymerization, the more the PPC M_n(experimental)/M_n(calculated) ratio decreases, consistent with the cocatalyst anion having an initiator role. Increasing the relative loading of [PPN]Cl generally increases the copolymerization rate, however, a loss in selectivity for PPC over PC is also observed (Figure 1.9). To further support that both the catalyst axial ligand and cocatalyst anion is capable of initiation, we prepared low M_n PPC with two different catalyst/cocatalyst combinations: (*R,R*)-

(salcy)CoOBzF$_5$/[PPN]Cl and (*R,R*)-(salcy)CoCl/[PPN][OBzF$_5$]. The isolated PPC from either system showed UV activity by the gel permeation chromatography (GPC) UV detector, and had a ^{19}F NMR spectrum consistent with OBzF$_5$ end groups (^{19}F NMR (470 MHz, ref C_6F_6 (–162.90 ppm)) resonances at δ –138 (m), –149 (m), –161 (m) ppm). Based on these results, we suggest that initiation occurs from both the catalyst axial ligand and the anion from the organic-based, ionic cocatalyst and that two polymer chains can propagate per one cobalt center (Scheme 1.7). This mechanistic scheme is consistent with that proposed by both Inoue and Lu in similar systems.[4, 21, 25]

As previously noted, the ^{13}C{^{1}H} NMR spectrum of PPC generated using catalyst system (*R,R*)-(salcy)CoOBzF$_5$/[PPN]Cl and *rac*-PO/CO_2 at 22 °C, has a large HT [*mm*] resonance, indicative of iso-enriched polymer. In an attempt to further increase the stereoselectivity of this catalyst, we lowered the copolymerization temperature. The effects of temperature on the selectivity of catalyst system (*R,R*)-(salcy)CoOBzF$_5$/[PPN]Cl for (*S*)- over (*R*)-PO are listed in Table 1.4. In each case, the PPC formed was decomposed to PC while conserving all stereocenters, and the k_{rel} for (*S*)- over (*R*)-PO was calculated. When the *rac*-PO/CO_2 copolymerization was carried out at 22 °C, catalyst system (*R,R*)-(salcy)CoOBzF$_5$/[PPN]Cl exhibits a k_{rel} = 5.1 (entry 1). Lowering the temperature to 0 °C and -20 °C, increases the selectivity for (*S*)- over (*R*)-PO, with k_{rel}s of 6.6 and 9.7, respectively (entries 2 and 3). The PPC formed in the later case shows a ^{13}C{^{1}H} NMR spectrum with [*rr*], [*rm*], and [*mr*] triad resonances that are approximately equal in magnitude and are each close to 1/6th that of the [*mm*] shift (Figure 1.10). This [*rr*]:[*rm*]:[*mr*]:[*mm*] ratio of 1:1:1:6 supports that the polymerization proceeds via an enantiomorphic-site control mechanism. Using the enantiomorphic-site expressions in the Bovey formalism for PPC triad sequences,[36] we calculate [*mm*] = 0.70, [*rr*] = 0.10, [*rm*] = 0.10, and [*mr*] = 0.10,

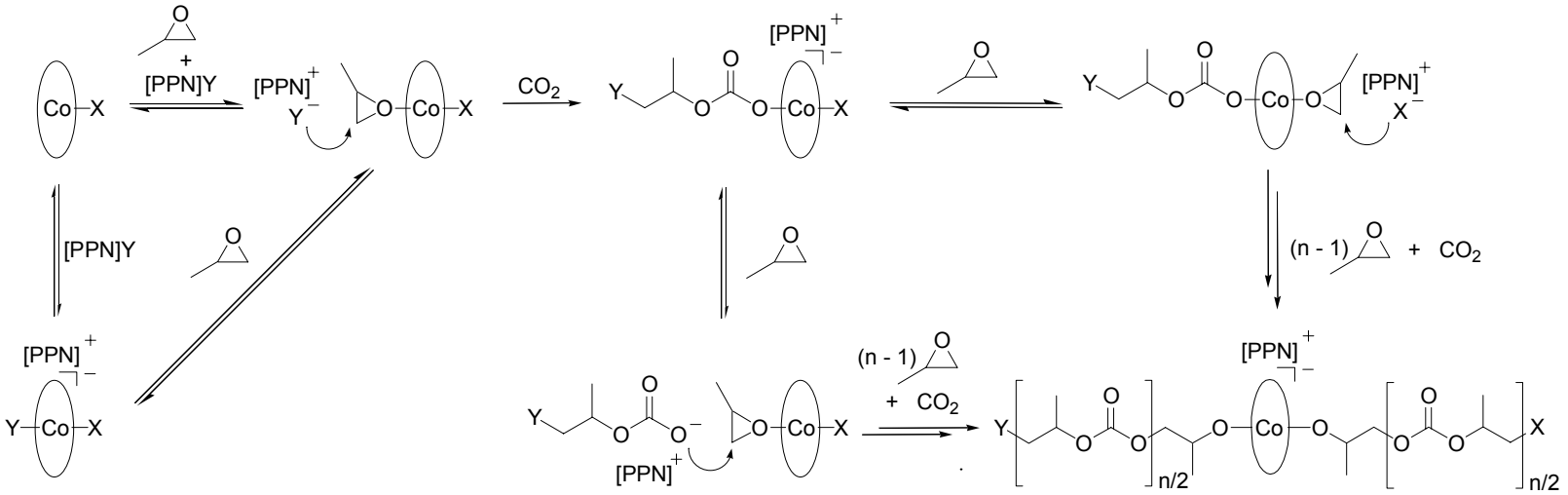

Scheme 1.7. Proposed mechanism for PO/CO_2 copolymerization using catalyst system (*R,R*)-(salcy)CoX/[PPN]Y (X, Y = halide, carboxylate, or polymer).

Table 1.4. Temperature effects on the stereochemistry of PPC formed.[a]

Entry	T (°C)	Time (h)	PPC Yield (%)	%*ee* (*S*)- [b]	α[c]	k_{rel}[d]	[*mm*] Calc.(%),Obs.(%)[e]	[*mr*] + [*rm*] Calc.(%),Obs.(%)[e]	[*rr*] Calc.(%),Obs.(%)[e]
1	22	1.0	30	60	0.80	5.1	52, 51	32, 32	16, 17
2	0	6.0	26	68	0.84	6.6	60, 58	27, 27	13, 15
3	-20[f]	10.0	19	78	0.89	9.7	70, 64	20, 24	10, 12
4	-20 → 20[fg]	3.0	39	64	0.82	6.7	55, 51	30, 32	15, 17

[a] Copolymerizations run neat with [*rac*-PO]:[Co]:[[PPN]Cl] = 1000:1:1. Entries 1 – 2 run with 100 psi CO_2, entries 3 – 4 run with 80 psi of CO_2. [b] Determined by decomposition of PPC to PC while maintaining all stereocenters and GC analysis of PC formed. [c] Enantioface selectivity parameter for the (*S*)-stereocenter of the enantiomorphic-site. [d] Relative rate constant for enchainment of (*S*)- over (*R*)-PO. [e] % HT tetrads as calculated from the enantiomorphic-site expressions in the Bovey formalism: $[mm] = \alpha^3 + (1-\alpha)^3$; $[mr] = [rm] = [rr] = \alpha^2(1-\alpha) + \alpha(1-\alpha)^2$ and % HT tetrads as integrated following deconvolution of the quantitative $^{13}C\{^1H\}$ NMR ($CDCl_3$, 125 MHz, d_1 = 10s) spectra. [f] +/- 8 °C. [g] Warmed from -20 °C to 22 °C over 3 h.

consistent with what we integrate following deconvolution of the quantitative $^{13}C\{^1H\}$ NMR spectrum. Finally, when the *rac*-PO/CO_2 copolymerization is initially cooled to -20 °C and then slowly warmed to 22 °C over 3 h, we calculate a k_{rel} of 6.7. Notably, (*R,R*)-(salcy)CoOBzF_5/[PPN]Cl is less selective for (*S*)- over (*R*)-PO when the reaction is not maintained at -20 °C, precluding an initiation effect.

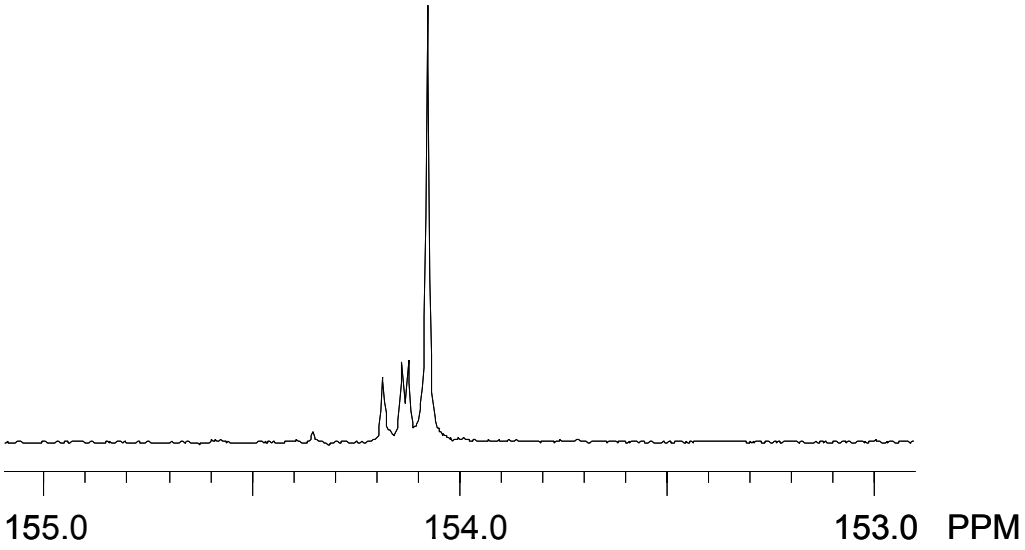

Figure 1.10. Carbonyl region of the quantitative $^{13}C\{^1H\}$ NMR spectrum ($CDCl_3$, 125 MHz, d_1 = 10s) of PPC generated using catalyst system (*R,R*)-(salcy)CoOBzF_5/ [PPN]Cl and *rac*-PO/CO_2 at -20 °C.

1.4 Addition of various organic-based, ionic cocatalysts

The mechanism we propose for the (*R,R*)-(salcy)CoOBzF_5/[PPN]Cl catalyzed *rac*-PO/CO_2 copolymerization highlights that $[PPN]^+$ helps to stabilize the propagating species and/or the cobaltate anion formed and that Cl^- is involved in polymer initiation (Scheme 1.7). In accordance with this scheme, we reason that the ideal cocatalyst

consists of a bulky, organic-based, ionic cation with a delocalized positive charge and a nucleophilic anion with a poor leaving ability. To test this generalization, we carried out the (*R,R*)-(salcy)CoOBzF$_5$ catalyzed *rac*-PO/CO$_2$ copolymerization in combination with various organic-based, ionic cocatalysts (Figure 1.11).[22] Application of the series, [PPN]Y (Y = Cl^-, $OBzF_5^-$, Br^-, BPh_4^-) revealed activities where $OBzF_5^-$ > Cl^- > Br^-, whereas the non-nucleophilic BPh_4^- was ineffective. This is similar to the trend we observed using (*R,R*)-(salcy)CoX/[PPN]Cl with different catalyst axial ligands, X, and is consistent with the cocatalyst anion capable of initiation. In the case of [PPN]Br, selectivity for PPC over PC was greatly reduced, a consequence of the good leaving ability of Br^-.

To study the role of the cocatalyst cation, we investigated the series, ACl (A = $[PPN]^+$, $[PPh_4]^+$, $[PPh_3(Me)]^+$, and $[n\text{-}Bu_4N]^+$) for *rac*-PO/CO$_2$ copolymerization when coupled with catalyst (*R,R*)-(salcy)CoOBzF$_5$. Similar to our results with [PPN]Cl, cocatalyst [PPh$_4$]Cl contributed to high activity with 97% selectivity for PPC over PC. Cocatalyst [PPh$_3$(Me)]Cl, however, had little rate enhancement capability. With this cocatalyst, it is plausible that an ylid is formed in situ, participating in side reactions detrimental to PPC formation. Finally, the ammonium salt [*n*-Bu$_4$N]Cl is less effective than [PPN]Cl, although highly selective for PPC, with >99:1 PPC:PC formed. Overall, our studies support that cocatalysts comprised of a bulky cation with a delocalized positive charge and a nucleophilic anion with poor leaving ability is the most effective for PO/CO$_2$ copolymerization rate enhancement; results consistent with those presented by Lu and coworkers with similar systems.[21]

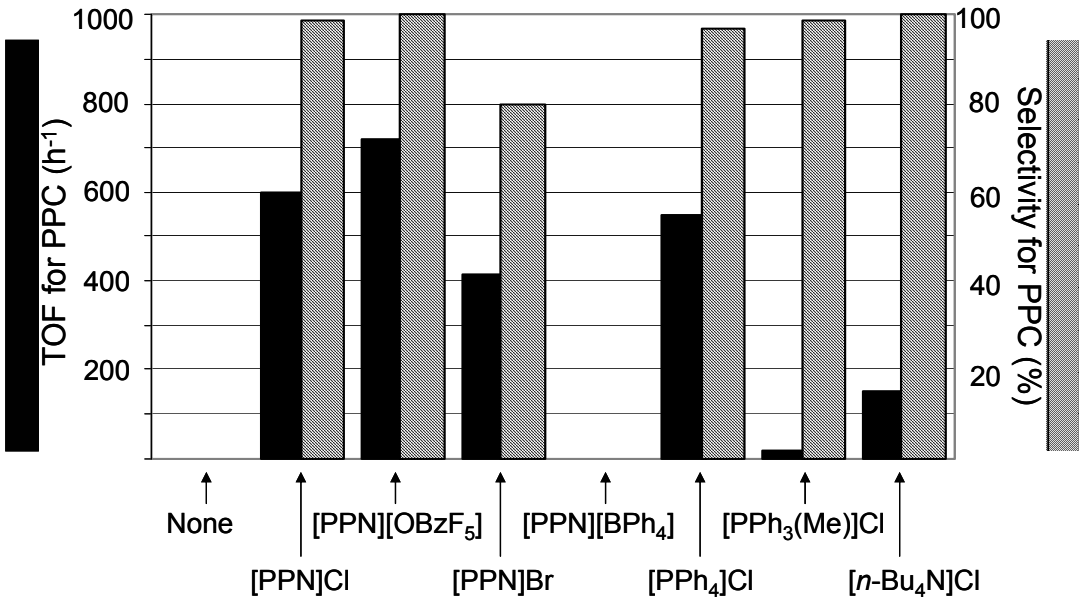

Figure 1.11. Influence of various ionic-based, organic cocatalysts on (*R,R*)-(salcy)CoOBzF$_5$ catalyzed *rac*-PO/CO$_2$ copolymerization rate and selectivity for PPC over PC. Copolymerizations run neat with [*rac*-PO]:[Co]:[cocatalyst] = 1000:1:1 at 22 °C with 100 psi of CO$_2$ and carried out to < 40% conversion. All PPC contains ≥ 99% carbonate linkages with $M_w/M_n \leq 1.26$ and ≥ 91% HT connectivity. Turnover frequency for PPC = (mol PO/(mol Co · h)).

1.5 Addition of Lewis basic cocatalysts

The addition of Lewis basic cocatalysts to epoxide/CO$_2$ copolymerization with porphyrin or salen-type metal catalysts has provided for enhanced catalytic activities in a variety of systems.[15-18, 21-24, 27, 29-31] In some cases, it has been suggested that the Lewis base directly coordinates to the catalyst, increases the electron density on the metal, and labilizes the species *trans* to it (Scheme 1.8).[15-18, 23, 24, 30, 31] Recently, Darensbourg and coworkers have shown that the relative loading as well as the steric and electronic nature of nitrogen-donor, Lewis basic cocatalysts have a large influence on catalyst activity using chromium-supported salen catalysts for CHO/CO$_2$ copolymerization.[27] Furthermore, they observe that the success of the cocatalyst is related to its ability to resonance stabilize negative charge on the nitrogen-donor atom. Through use of in situ infrared monitoring of salen-Cr/DMAP (DMAP = 4-

(dimethylamino)pyridine) catalyzed CHO/CO_2 copolymerization, they initially observe shifts consistent with CO_2 inserting into a metal-amide bond, which later disappear as the reaction proceeds. Notably, this zwitterionic, CO_2-activated DMAP species has been previously proposed by Nguyen and coworkers,[37, 38] and is suspected to be capable of polymer initiation.[27]

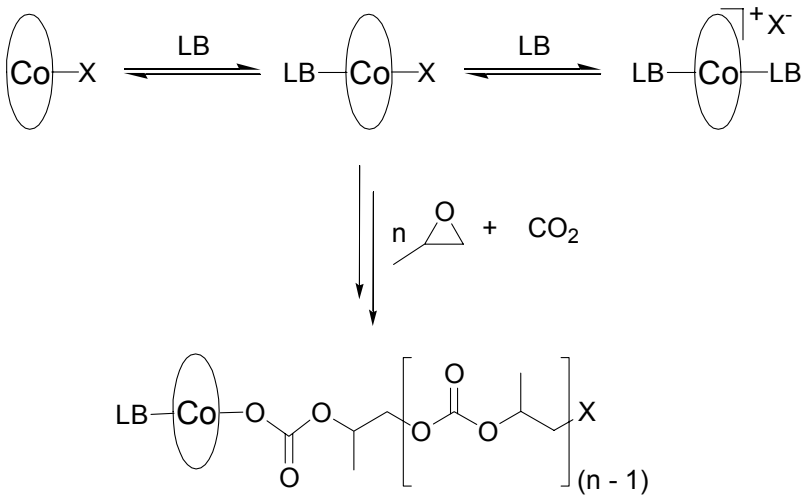

Scheme 1.8. A mechanism for (salen)CoX catalyzed *rac*-PO/CO_2 copolymerization in the presence of Lewis basic cocatalysts.

Nguyen and coworkers investigated the addition of *N*,*N*-dimethylaminoquinoline (DMAQ) or (*R*)-(+)-4-(dimethylamino)pyridinyl(pentaphenylcyclopentadienyl)iron (DMAP*) to [(*R*,*R*)-Co^{III}(salen)]$^+$-based complexes for *rac*-PO/CO_2 copolymerization.[18] They observe the highest activities when 2 equivalents of cocatalyst are used, with no obvious relationship between the nature of the catalyst counteranion and catalytic activity. In these systems, the highest activities were realized using [(*R*,*R*)-Co^{III}(salen)][NO_3] complexes with DMAQ or DMAP*, despite the non-nucleophilic nature of the catalyst

counterion. In all cases, the M_n values of the PPCs obtained are lower than the corresponding theoretical values. Similarly, Lu and coworkers have shown that the addition of the sterically hindered, 7-methyl-1,5,7-triazabicyclo[4.4.0]dec-5-ene (MTBD) to catalyst *N*,*N*′-bis(3,5-di-*tert*-butylsalicylidene)-1*R*,2*R*-cyclohexanediimino(2,4-dinitrophenoxy)cobalt(III) [(*R,R*)-(salcy)CoX; X = 2,4-dinitrophenoxy] yields high activities for PO/CO_2 copolymerization, whereas this catalyst coupled to the nonsterically hindered *N*-methylimidazole is inactive. When adding MTBD to catalyst (*R,R*)-(salcy)CoX (X = 2,4-dinitrophenoxy), the number of PPC chains (based on the observed vs. calculated M_n values) did not depend on the cobalt complex loading, but was instead a function of the applied MTBD concentration. Use of the catalyst system (*R,R*)-(salcy)CoX/MTBD (X = ClO_4^-) was successful for *rac*-PO/CO_2 copolymerization. Consistent with work presented by Nguyen,[18] the non-nucleophilic nature of the catalyst counterion was not detrimental to polymer formation.[21] Using in situ ESI-MS, for the (*R,R*)-(salcy)CoX/MTBD (X = 2,4-dinitrophenoxy) catalyzed PO/CO_2 copolymerization revealed the species [$^-$OCH(CH_3)CH_2-(CO_2-*alt*-PO)$_n$-MTBD$^+$ + H^+] which is found to move to the higher *m*/*z* region throughout the reaction. Although the species [$^-$OOCOCH(CH_3)CH_2-(CO_2-*alt*-PO)$_n$-MTBD$^+$] is more likely to dissociate from the cobalt than the propagating alkoxide, this ion is unstable in the absence of free CO_2 and is not found in the mass spectrum. Based on their results, Lu proposes a mechanism where the Lewis base has an initiator role, and additionally suggests that the propagating carboxylate dissociates from the active cobalt catalyst throughout the copolymerization.

To explore the effects of Lewis base cocatalysts using our catalyst systems, we investigated a series of amines and pyridinium compounds in conjunction with catalyst (*R,R*)-(salcy)CoOBzF_5 (Figure 1.12).[22] When added to (*R,R*)-(salcy)CoOBzF_5, triethylamine and *n*-trioctylamine are effective cocatalysts achieving TOFs of 190 h^{-1}

and 175 h^{-1}, respectively. The similarity in activity suggests that the alkyl length of the amine cocatalyst has little influence on its performance. Interestingly, when increasing relative amounts of *n*-trioctylamine are applied, the M_n values of the resultant PPCs decrease (Figure 1.13). This is consistent with the Lewis basic cocatalyst capable of initiation and/or reacting with CO_2, a similar scheme to that proposed by Lu (Scheme 1.9a)[21] and Darensbourg (Scheme1.9b).[27]

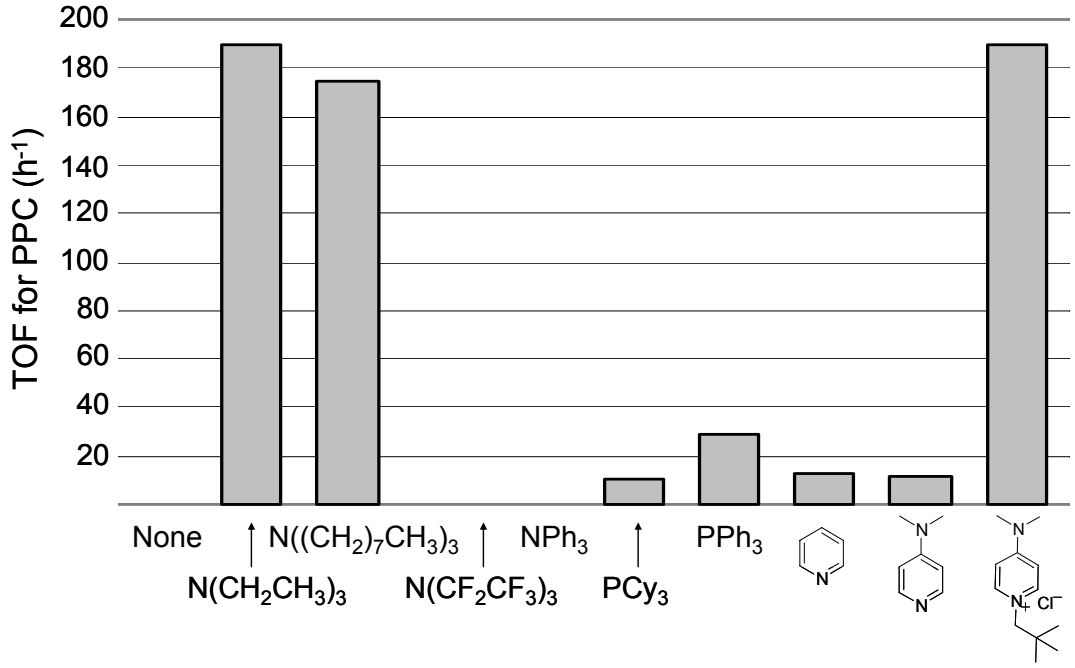

Figure 1.12. Influence of Lewis basic cocatalysts on (*R,R*)-(salcy)CoOBzF_5 catalyzed *rac*-PO/CO_2 copolymerization. Copolymerizations run neat with [*rac*-PO]:[Co]:[cocatalyst] = 1000:1:1 at 22 °C with 100 psi of CO_2 and carried out to < 40% conversion. All PPC contains ≥ 99% carbonate linkages with $M_w/M_n \leq 1.19$ and ≥ 92% HT connectivity and ≥ 99:1 selectivity for PPC over PC. Turnover

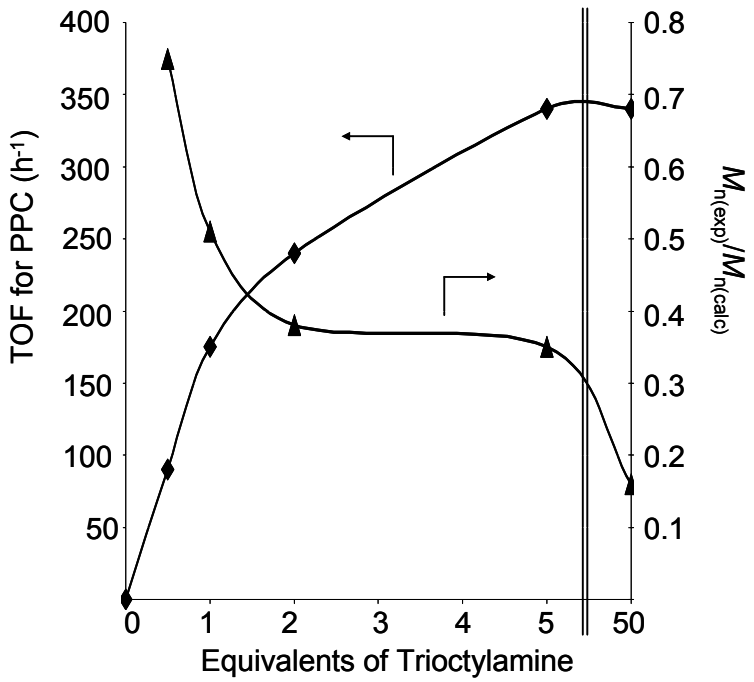

Figure 1.13. Effect of trioctylamine loading on (*R,R*)-(salcy)CoOBzF$_5$ catalyzed *rac*-PO/CO_2 copolymerization activity and M_n values of the PPC formed. Copolymerizations run in neat *rac*-PO with [PO]:[Co] = 1000:1 at 22 °C with 100 psi of CO_2 and carried out to < 40% conversion. Turnover frequency for PPC = (mol PO/(mol Co · h)). $M_{n(exp)}/M_{n(calc)}$ = ratio of the experimental M_n value to the corresponding calculated M_n value based on catalyst loading.

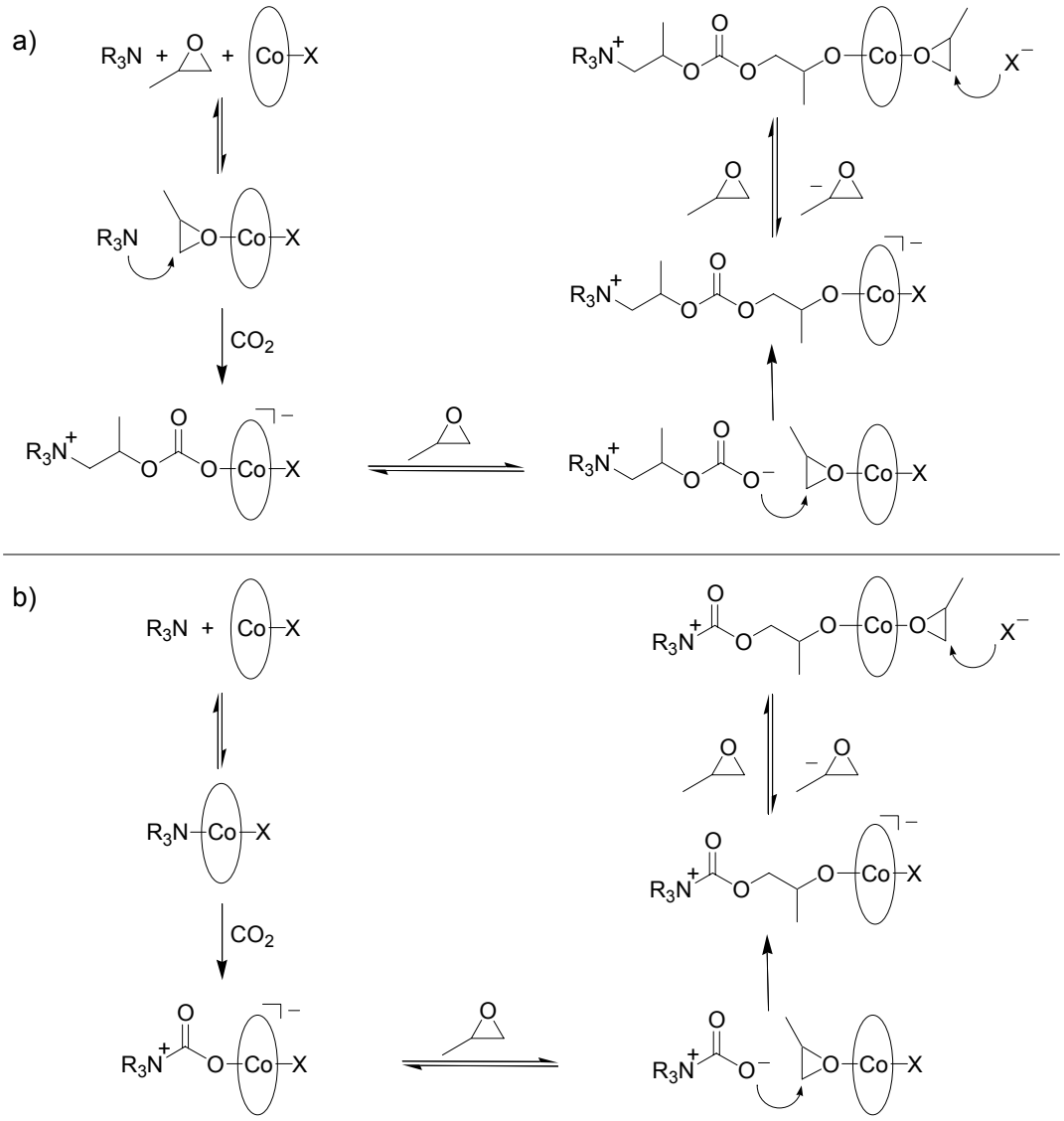

Scheme 1.9. Mechanism for (salen)CoX (X = halide or carboxylate) catalyzed *rac*-PO/CO_2 copolymerization in the presence of a Lewis base cocatalyst (NR_3, R = alkyl): a) The Lewis base directly ring-opens the cobalt-bound PO and b) Insertion of CO_2 into the cobalt-nitrogen bond prior to PO ring-opening.

When perfluorotriethylamine ($N(CF_2CF_3)_3$) is applied, (*R,R*)-(salcy)$CoOBzF_5$ has no copolymerization activity, presumably due to the very weak Lewis basicity and/or nucleophilicity of this cocatalyst. This is also the case when the sterically bulky triphenylamine (NPh_3), triphenylphosphine (PPh_3), or tricyclohexylphosphine (PCy_3) cocatalysts are used. When pyridine or DMAP cocatalysts are employed, (*R,R*)-(salcy)$CoOBzF_5$ shows little overall activity; results quite different than those observed for chromium-based systems.[27] Notably, these cocatalysts are capable of irreversible coordination to the cobalt catalyst, possibly leading to its inactivation. Finally, a cocatalyst comprised of both a Lewis base and an organic-based, ionic cation yields activities reminiscent of the organic-based, ionic cocatalysts, suggesting that the ion-assisted copolymerization is the prevailing mechanism.

Overall, a delicate interplay between Lewis basicity, steric bulk, and reversibility of coordination make the electron rich alkyl amines the most effective Lewis basic cocatalysts, although they are inferior to the organic-based, ionic cocatalysts $[Ph_4P]Cl$, or [PPN]Y (Y = Cl or $OBzF_5$). Furthermore, we suspect that both the coordination of the Lewis base to the metal center (Scheme 1.8), and/or initiation is viable (Scheme 1.9) where a competition between mechanisms is determined by the steric and electronic environment around the cocatalyst donor atom.

1.6 Stereoselective CHO/CO_2 copolymerization

The asymmetric copolymerization of CHO and CO_2 has been achieved by both Nozaki and in our group, using zinc-based catalysts with chiral aminoalkoxy and imine-oxazoline ligands, respectively (Figure 1.3).[7-11] In each case, the desymmetrization and coupling of the *meso* epoxide with CO_2 yields isotactic PCHC with an *ee* > 70%. The classification of this polymer was described in earlier reports; both we and Nozaki have assigned the carbonyl region of the $^{13}C\{^1H\}$ NMR spectrum for isotactic PCHC.[7, 11] The characterization of isotactic PCHC was further

corroborated using statistical methods,[11] and additionally, Nozaki has identified the resonances corresponding to [*mmm*] and [*rrr*] tetrad sequences by synthesizing model PCHC oligomers.[39]

As previously described, we have achieved a variety of PPC microstructures using catalysts (salcy)CoX (X = halide or carboxylate) for PO/CO_2 copolymerization.[19] Moreover, we were eager to apply these chiral catalysts to CHO/CO_2 copolymerization, with the hope of uncovering an enantioselective catalyst for isotactic PCHC. Surprisingly, when we applied any of the (*R,R*)-(salcy)CoX (X = Cl, Br, I, $OBzF_5$, OAc) complexes to CHO/CO_2 copolymerization at high CO_2 pressures (800 psi), we observed PCHCs with unprecedented $^{13}C\{^1H\}$ NMR spectra.[28] Although the ^1H NMR spectra of these polymers were consistent with previously characterized PCHC,[40] the $^{13}C\{^1H\}$ NMR spectra revealed strong contributions correlating to *r*-centered tetrads, indicative of *syndiotactic* PCHC (Figure 1.14).

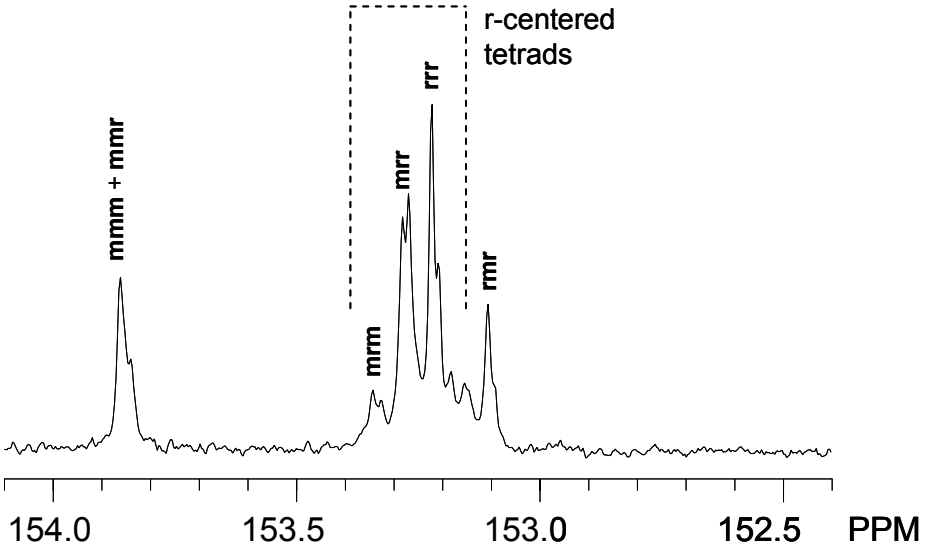

Figure 1.14. Carbonyl region of the quantitative $^{13}C\{^1H\}$ NMR spectrum of syndio-enriched PCHC generated using catalyst (*R,R*)-(salcy)CoI for CHO/CO_2 copolymerization.

We initially suspected that a chain-end control mechanism prevailed with the (*R,R*)-(salcy)CoX systems, a pathway not observed in the previously studied zinc-based catalysts. To test this possibility, we prepared PCHC from CHO and CO_2 using a series of chiral, racemic, and achiral (salen)CoX complexes, and compared the ligand structure to the tacticity of the PCHC synthesized (Figure 1.15).

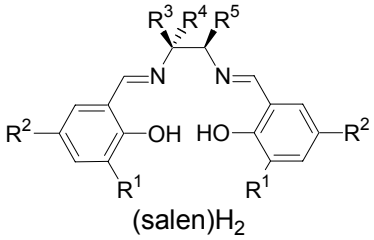

(salen)H_2

Ligand	R^1	R^2	R^3	R^4	R^5
(salen-**1**)H_2	^{t}Bu	^{t}Bu	H	*trans* -$(CH_2)_4$-	
(salen-**2**)H_2	^{t}Bu	^{t}Bu	Me	H	H
(salen-**3**)H_2	^{t}Bu	^{t}Bu	H	H	H
(salen-**4**)H_2	Me	H	H	*trans* -$(CH_2)_4$-	
(salen-**5**)H_2	cumyl	cumyl	H	*trans* -$(CH_2)_4$-	

(salen-**1**)H_2 = (salcy)H_2

Figure 1.15. (Salen)H_2 ligands used in the synthesis of (salen)CoX complexes for CHO/CO_2 copolymerization. Cumyl = α,α'-dimethylbenzyl.

Table 1.5. (Salen)CoX (X = Br, $OBzF_5$) catalyzed CHO/CO_2 copolymerization with and without [PPN]Cl cocatalysts.[a]

Entry	Catalyst	Cocatalyst	Time (h)	CO_2 Pressure (psi)	PCHC Yield[b] (%)	TOF[c] (h^{-1})	*r*-Centered Tetrads[d] (%)
1	(*R,R*)-(salen-**1**)CoBr	none	20	800	66	16	66
2	*rac*-(salen-**1**)CoBr	none	20	800	64	16	78
3	(salen-**2**)CoBr	none	20	800	90	22	75
4	*rac*-(salen-**3**)CoBr	none	20	800	87	22	80
5	*rac*-(salen-**3**)CoBr	none	3	800	59	98	81
6	*rac*-(salen-**3**)CoOBzF_5	none	3	800	56	93	76
7	*rac*-(salen-**4**)CoOBzF_5	none	3	800	19	32	50
8	*rac*-(salen-**3**)CoOBzF_5	none	48	100	35[e]	4	60
9	*rac*-(salen-**3**)CoOBzF_5	[PPN]Cl	2	100	18	90	56
10	(*R,R*)-(salen-**1**)CoOBzF_5	[PPN]Cl	2	100	32	160	49
11[f]	(*R,R*)-(salen-**1**)CoOBzF_5	[PPN]Cl	1	100	44	440	47
12	(*R,R*)-(salen-**5**)CoBr	none	72	100	32	2	35

[a] Entries 1 – 8 and 12 run neat at 22 °C with [CHO]:[Co] = 500:1. Entries 9 – 11 run neat at 22 °C with [CHO]:[Co]:[[PPN]Cl] = 1000:1:1. In all cases, cyclohexene carbonate is not observed and PCHCs have ≥ 96% carbonate linkages as determined by ^{1}H NMR spectroscopy ($CDCl_3$, 300 MHz). [b] Based on isolated PCHC yield. [c] Turnover frequency for PCHC = (mol CHO/(mol Co · h)). [d] Determined by quantitative $^{13}C\{^1H\}$ NMR spectroscopy ($CDCl_3$, 125 MHz, d_1 = 10s). [e] 80% Carbonate linkages. [f] 70 °C.

The PCHC formed using catalyst (*R,R*)-(salen-**1**)CoBr ((salen-**1**) = salcy) has 66% *r*-centered tetrads; an approximate value acquired from integration of the deconvoluted, quantitative $^{13}C\{^1H\}$ NMR spectrum of this polymer (Table 1.5, entry 1). Interestingly, application of the racemic analogue, *rac*-(salen-**1**)CoBr, generates a more syndiotactic PCHC with 78% *r*-centered tetrads (entry 2), where the achiral (salen-**2**)CoBr catalyst yielded PCHC with 75% *r*-centered tetrads (entry 3). Notably, a chiral ligand is not a necessary condition for the generation of syndiotactic PCHC, evocative of a chain-end control mechanism. Finally, use of *rac*-(salen-**3**)CoBr forms the most syndiotactic PCHC we observe, with 80% *r*-centered tetrads (entry 4).

With the more active (salen-**2**)CoBr and *rac*-(salen-**3**)CoBr catalysts, PCHC is obtained in high yields (87%) after prolonged reaction times. We suspect that the at high CO_2 pressures (800 psi), CO_2 functions as a solvent, allowing for unusually high PCHC conversion. When the CHO/CO_2 copolymerization is quenched after only 3 h using catalyst *rac*-(salen-**3**)CoBr, we measure a TOF = 98 h^{-1} with no loss of syndioselectivity (entry 5).

When the steric bulk of the salen ligand is greatly reduced, the resultant complex *rac*-(salen-**4**)CoBr is too soluble in pentane to purify by standard filtration methods, whereas the less soluble *rac*-(salen-**4**)CoOBzF_5 is readily synthesized. It is notable that catalysts *rac*-(salen-**3**)CoX (X = OBzF_5, Br) show similar CHO/CO_2 copolymerization behavior, with only a slight loss in syndioselectivity when X = OBzF_5 is used (Table 1.5, entry 6 and Figure 1.16a). When the *rac*-(salen-**4**)CoOBzF_5 is applied to CHO/CO_2 copolymerization, all stereochemical direction is lost, generating *atactic* PCHC. This suggests that moderate ligand steric bulk is necessary for a chain-end control mechanism to operate (Table 1.5, entry 7 and Figure 1.16c).

When the *rac*-(salen-**3**)CoOBzF_5 catalyzed CHO/CO_2 copolymerization is carried out at low CO_2 pressures, catalyst activity is greatly reduced from that observed using 800 psi. Interestingly, the selectivity for syndiotactic PCHC was also compromised under these conditions (entry 8). Addition of cocatalyst [PPN]Cl to this copolymerization increased the rate somewhat, but further reduced selectivity for syndiotactic PCHC (entry 9). When we applied the most active PO/CO_2 copolymerization catalyst system ((*R,R*)-(salcy)CoOBzF_5/[PPN]Cl), we observe a TOF = 160 h^{-1} for atactic PCHC (entry 10). Notably, this is dissimilar from results presented by Lu, concerning (*R,R*)-(salcy)CoX/[PPN]Cl (X = 2,4-dinitrophenoxy) for the synthesis of isoenriched PCHC with an *ee* of 36.6%.[21] Interestingly, we observed that heating the CHO/CO_2 copolymerization led to increased activity, without loss in

selectivity for PCHC or catalyst decomposition (entry 11). We suspect that [PPN]Cl stabilizes the active cobalt catalyst even at high temperatures; an effect limited to CHO/CO_2 polymerization.

Based on our results, we suggest a chain-end control mechanism for CHO/CO_2 copolymerization is no longer operable at low CO_2 pressures. As such, we applied our most sterically bulky catalyst, (*R,R*)-(salen-**5**)CoBr, when using only 100 psi of CO_2 in an effort to invoke an enantiomorphic-site control mechanism for isotactic PCHC. Indeed, the (*R,R*)-(salen-**5**)CoBr catalyzed CHO/CO_2 copolymerization at low CO_2 pressures (100 psi), produced *isoenriched* PCHC with 65% *m*-centered tetrads and 99% carbonate incorporation (Table 1.5, entry 12 and Figure 1.16d). When this PCHC was broken down to cyclohexene diol while maintaining all stereocenters,[40] we observed an (*R,R*) to (*S,S*) ratio of 78:22 (*ee* = 56%) as determined by GC.

In summary, enantiomerically pure, racemic, and achiral (salen)CoX catalysts are all syndioselective for CHO/CO_2 copolymerization at high CO_2 pressures (800 psi), supporting that monomer enchainment proceeds by a chain-end control mechanism. When low pressures are used (100 psi), an enantiomorphic-site control mechanism becomes competitive, whereas use of a chiral sterically bulky catalyst is selective for isotactic PCHC. Finally, addition of [PPN]Cl to selective (salen)CoOBzF_5 complexes increases copolymerization rates, and can be carried out at 70 °C for optimal copolymerization activity.

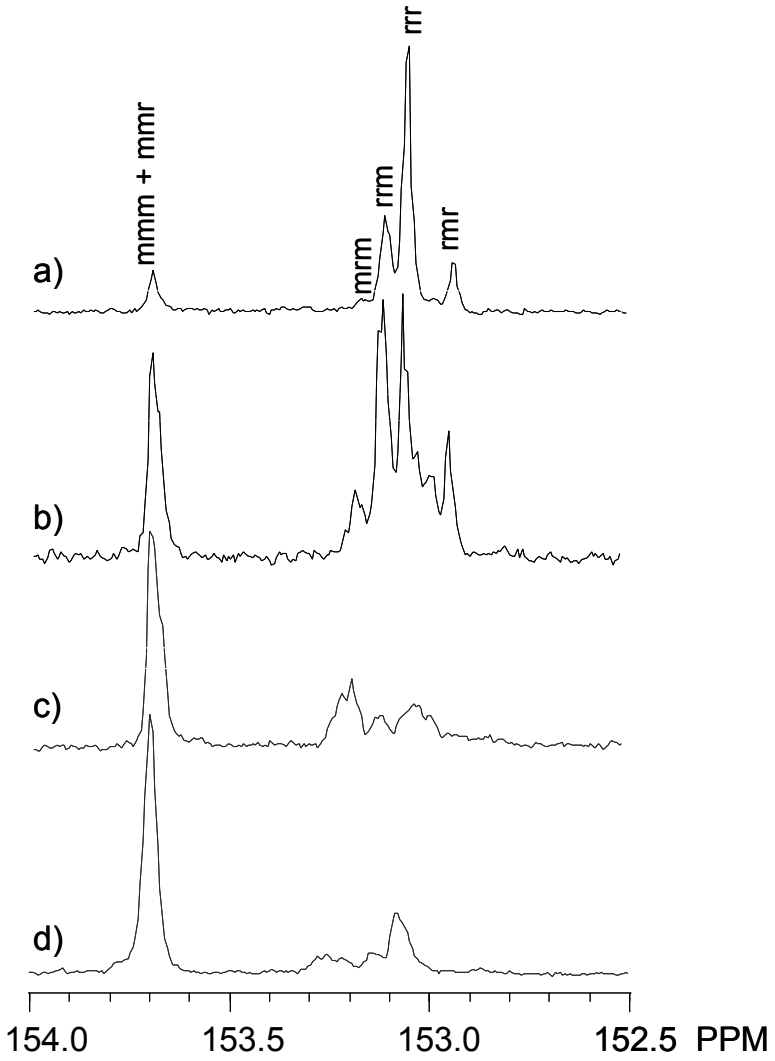

Figure 1.16. Carbonyl region of the quantitative $^{13}C\{^{1}H\}$ NMR spectra ($CDCl_3$, 125 MHz, d_1 = 10s) of PCHCs generated using CHO/CO_2 (800 psi) with catalyst a) *rac*-(salen-**3**)$CoOBzF_5$, b) (*R,R*)-(salen-**1**)$CoOBzF_5$, c) *rac*-(salen-**4**)$CoOBzF_5$ and d) CHO/CO_2 (100 psi) with catalyst (*R,R*)-(salen-**5**)CoBr.

1.7 Concluding remarks

A growing area in CO_2 chemistry is the development of catalysts for the alternating copolymerization of epoxides and CO_2 to form polycarbonates. Advances over the last forty years have led to high catalytic activities for this transformation; however, control of polymer microstructure is seldom attained. Notably, the

correlation between a polymer's main-chain structure and its physical properties has inspired the pursuit of regio- and stereoselective epoxide/CO_2 copolymerization catalysts. Furthermore, since Jacobsen and coworkers have reported chiral (salen)Co^{III} carboxylates for the hydrolytic kinetic resolution of epoxides with remarkable selectivities and efficiencies,[13] the application of similar systems for epoxide/CO_2 copolymerization has received much attention.

As described above, we have developed (salen)CoX (X = halide or carboxylate) catalysts for both PO/CO_2 and CHO/CO_2 copolymerization. Through adjustment of the reaction environment and catalyst optimization we were able to maximize catalytic activity and selectivity for the generation of highly alternating, regioregular PPC with controlled molecular weight and no detectable PC byproduct. By varying catalyst and PO stereochemistry, we observed pronounced alterations in both catalytic activity and PPC microstructure, and describe the first example syndio-enriched PPC. The addition of organic-based, ionic or Lewis basic cocatalysts to (*R,R*)-(salcy)CoOBzF_5 has resulted in enhanced PO/CO_2 copolymerization rates, achieving highly alternating, regioregular PPC. When applied to CHO/CO_2 copolymerization, (salen)CoX (X = Br, OBzF_5) catalysts provide a viable route to syndiotactic PCHC, a previously unreported PCHC microstructure. The structural properties of the salen ligands supporting these catalysts dictate the syndiotacticity of the resultant PCHC, a correlation which we attribute to a competition of chain-end and enantiomorphic-site control mechanisms.

Our future goals in catalyst development are centered on improved systems for PO/CO_2 kinetic resolution polymerization as well as for CHO/CO_2 asymmetric synthesis polymerization. To achieve this, we will pursue more detailed mechanistic studies in order to identify the means of stereocontrol in each system. Furthermore, we

are currently investigating the structure-property relationship of polycarbonates with varying microstructures, with the purpose of installing improved properties.

1.8 References

(1) (a) Inoue, S.; Koinuma H.; Tsuruta, T. *J. Polym. Sci. Polym. Phys.* **1969**, *7*, 287 - 292. (b) Inoue, S.; Koinuma, H.; Tsuruta, T. *Makromol. Chem.* **1969**, *130*, 210 - 220.

(2) (a) Arakawa, H. *et al. Chem. Rev.* **2001**, *101*, 953-996. (b) Musie, G.; Wei, M.; Subramaniam, B.; Busch, D. H. *Coord. Chem. Rev.* **2001**, *219*, 789-820. (c) Cooper, A. I. *J. Mater. Chem.* **2000**, *10*, 207-234. (d) Bolm, C.; Beckmann, O.; Dabard, O. A. G. *Angew. Chem. Int. Ed.* **1999**, *38*, 907-909. (e) Yin, X. L.; Moss, J. R. *Coord. Chem. Rev.* **1999**, *181*, 27-59. (f) Gibson, D. H. *Chem. Rev.* **1996**, *96*, 2063-2095. (g) Leitner, W. *Coord. Chem. Rev.* **1996**, *153*, 257-284. (h) Leitner, W. *Angew. Chem. Int. Ed.* **1995**, *34*, 2207-2221. (i) Jessop, P. G.; Ikariya, T.; Noyori, R. *Chem. Rev.* **1995**, *95*, 259-272.

(3) Allen, S. D. PhD Dissertation, Cornell University, May **2004** and references therein.

(4) For reviews on epoxide/CO_2 copolymerizations, see: (a) Ochiai, B.; Endo, T. *Prog. Polym. Sci.* **2005**, *30*, 183 - 215. (b) Moore; D. R.; Coates, G. W. *Angew. Chem. Int. Ed.* **2004**, *43*, 6618 - 6639. (c) Sugimoto H.; Inoue S. *J. Polym. Sci. Polym. Chem.* **2004**, *42*, 5561 - 5573. (d) Darensbourg, D. J.; Mackiewicz, R. M.; Phelps, A. L.; Billodeaux, D. R. *Acc. Chem. Res.* **2004**, *37*, 836 - 844. (e) Darensbourg, D. J.; Holtcamp, M. W. *Coord. Chem. Rev.* **1996**, *153*, 155 - 174. (f) Super, M. S.; Beckman, E. J. *Trends Polym. Sci.* **1997**, *5*, 236 - 240. (g) Kuran, W. *Prog. Polym. Sci.* **1998**, *23*, 919 - 992. (h) Aida, T.; Inoue, S. *Acc. Chem. Res.* **1996**, *29*, 39 - 48.

(5) For initial advances using zinc-based homogeneous catalysts for epoxide/CO_2 copolymerization see: (a) Darensbourg, D. J.; Holtcamp, M. W. *Macromolecules* **1995**, *28*, 7577-7579. (b) Darensbourg, D. J.; Holtcamp, M. W.; Struck, M. S.; Zimmer, S. A.; Niezgoda, S. A.; Rainey, J. B.; Robertson, J. D.; Draper, J. D.; Reibenspies, J. H. *J. Am. Chem. Soc.* **1999**, *121*, 107-116. (c) Super, M.; Berluche, E.; Costello, C.; Beckman, E. *Macromolecules* **1997**, *30*, 368-372. (d) Cheng, M.; Lobkovsky, E. B.; Coates, G. W. *J. Am. Chem. Soc.* **1998**, *120*, 11018-11019. (e) Cheng, M.; Moore, D. R.; Reczek, J. J.; Chamberlain, B. M.; Lobkovsky, E. B.; Coates, G. W. *J. Am. Chem. Soc.* **2001**, *123*, 8738-8749. (f) Moore, D. R.; Cheng, M.; Lobkovsky, E. B.; Coates, G. W. *Angew. Chem. Int. Ed.* **2002**, *41*, 2599-2602. (g) Moore, D. R.; Cheng, M.; Lobkovsky, E. B.; Coates, G. W. *J. Am. Chem. Soc.* **2003**, *125*, 11911-11924.

(6) Allen, S. D.; Moore, D. R.; Lobkovsky, E. B.; Coates, G. W. *J. Am. Chem. Soc.* **2002**, *124*, 14284-14285.

(7) Nozaki, K.; Nakano, K.; Hiyama, T. *J. Am. Chem. Soc.* **1999**, *121*, 11008-11009.

(8) Nakano, K.; Nozaki, K.; Hiyama, T. *J. Am. Chem. Soc.* **2003**, *125*, 5501-5510.

(9) Nakano, K.; Hiyama, T.; Nozaki, K. *Chem. Comm.* **2005**, 1871-1873.

(10) Nakano, K.; Kosaka, N.; Hiyama, T.; Nozaki, K. *Dalton Trans.* **2003**, 4039-4050.

(11) Cheng, M.; Darling, N. A.; Lobkovsky, E. B.; Coates, G. W. *Chem. Comm.* **2000**, 2007-2008.

(12) Inoue, S. *J. Polym. Sci. Polym. Chem.* **2000**, *38*, 2861-2871.

(13) Tokunaga, M.; Larrow, J. F.; Kakiuchi, F.; Jacobsen, E. N. *Science* **1997**, *277*, 936-938.

(14) Qin, Z.; Thomas, C. M.; Lee, S.; Coates, G. W. *Angew. Chem. Int. Ed.* **2003**, *42*, 5484-5487.

(15) Darensbourg, D. J.; Phelps, A. L. *Inorg. Chem.* **2005**, *44*, 4622-4629.

(16) Darensbourg, D. J.; Yarbrough, J. C.; Ortiz, C.; Fang, C. C. *J. Am. Chem. Soc.* **2003**, *125*, 7586-7591.

(17) Darensbourg, D. J.; Yarbrough, J. C. *J. Am. Chem. Soc.* **2002**, *124*, 6335-6342.

(18) Paddock, R. L.; Nguyen, S. T. *Macromolecules* **2005**, *38*, 6251-6253.

(19) Cohen, C. T.; Chu, T.; Coates, G. W. *J. Am. Chem. Soc.* **2005**, *127*, 10869-10878.

(20) Lu, X. B.; Wang, Y. *Angew. Chem. Int. Ed.* **2004**, *43*, 3574-3577.

(21) Following our work, Lu and coworkers published similar studies concerning (salen)CoX catalyzed PO/CO_2 copolymerization: Lu, X. B.; Lei, S.; Wang, Y. M.; Zhang, R.; Zhang, Y. J.; Peng, X. J.; Zhang, Z. C.; Li, B. *J. Am. Chem. Soc.* **2006**, *128*, 1664 - 1674.

(22) Cohen, C. T.; Coates, G. W. *J. Poly. Sci. Polym. Chem.* **2006**, *In Press*.

(23) Eberhardt, R.; Allmendinger, M.; Rieger, B. *Macromol. Rapid Commun.* **2003**, *24*, 194-196.

(24) Darensbourg, D. J.; Mackiewicz, R. M.; Rodgers, J. L.; Phelps, A. L. *Inorg. Chem.* **2004**, *43*, 1831-1833.

(25) (a) Aida, T.; Inoue, S. *J. Am. Chem. Soc.* **1985**, *107*, 1358-1365. (b) Aida, T.; Sanuki, K.; Inoue, S. *Macromolecules* **1985**, *18*, 1049-1055. (c) Aida, T.; Ishikawa, M.; Inoue, S. *Macromolecules* **1986**, *19*, 8-13. (d) Sugimoto, H.; Ohtsuka, H.; Inoue, S. *J. Polym. Sci. Polym. Chem.* **2005**, *43*, 4172-4186.

(26) Darensbourg, D. J.; Billodeaux, D. R. *Inorg. Chem.* **2005**, *44*, 1433-1442.

(27) Darensbourg, D. J.; Mackiewicz, R. M. *J. Am. Chem. Soc.* **2005**, *127*, 14026-14038.

(28) Cohen, C. T.; Thomas, C. M.; Peretti, K. L.; Lobkovsky, E. B.; Coates, G. W. *Dalton Trans.* **2006**, *1*, 237-249.

(29) Darensbourg, D. J.; Mackiewicz, R. M.; Billodeaux, D. R. *Organometallics* **2005**, *24*, 144-148.

(30) Darensbourg, D. J.; Mackiewicz, R. M.; Rodgers, J. L.; Fang, C. C.; Billodeaux, D. R.; Reibenspies, J. H. *Inorg. Chem.* **2004**, *43*, 6024-6034.

(31) Aida, T.; Inoue, S. *J. Am. Chem. Soc.* **1983**, *105*, 1304-1309.

(32) Nielsen, L. P. C.; Stevenson, C. P.; Blackmond, D. G.; Jacobsen, E. N. *J. Am. Chem. Soc.* **2004**, *126*, 1360-1362.

(33) Chisholm, M. H.; Navarro-Llobet, D.; Zhou, Z. P. *Macromolecules* **2002**, *35*, 6494-6504.

(34) Ovitt, T. M.; Geoffrey, W. C. *J. Am. Chem. Soc.* **2002**, *124*, 1316-1326.

(35) Lu, X. B.; Liang, B.; Zhang, Y. J.; Tian, Y. Z.; Wang, Y. M.; Bai, C. X.; Wang, H.; Zhang, R. *J. Am. Chem. Soc.* **2004**, *126*, 3732-3733.

(36) Coates, G. W. *Chem. Rev.* **2000**, *100*, 1223-1252.

(37) Paddock, R. L.; Hiyama, Y.; McKay, J. M.; Nguyen, S. T. *Tetrahedron Lett.* **2004**, *45*, 2023-2026.

(38) Paddock, R. L.; Nguyen, S. T. *Chem. Comm.* **2004**, 1622-1623.

(39) Nakano, K.; Nozaki, K.; Hiyama, T. *Macromolecules* **2001**, *34*, 6325-6332.

(40) Cheng, M. PhD Dissertation, Cornell University, May **2000**.